

Dynamics of Sorbed Molecules in Zeolites*

Scott M. Auerbach[†]

*Department of Chemistry and Department of Chemical Engineering,
University of Massachusetts, Amherst, MA 01003*

Fabien Jousse[‡] and Daniel P. Vercauteren

*Computational Chemical Physics Group, Institute for Studies in Interface Science,
Facultés Universitaires Notre-Dame de la Paix, Rue de Bruxelles 61, B-5000 Namur, Belgium*

Abstract

We explore recent efforts to model the dynamics of sorbed molecules in zeolites with either atomistic methods or lattice models. We discuss the assumptions underlying modern atomistic and lattice approaches, and detail the techniques and applications of modeling both rapid dynamics and activated diffusion. We summarize the major findings discovered over the last several years, and enumerate future needs for the frontier of modeling dynamics in zeolites.

*Submitted as a chapter in “*Computer Modelling of Microporous and Mesoporous Materials*,”
Editors C. R. A. Catlow, R. A. van Santen and B. Smit.

[†]Corresponding author; email: auerbach@chem.umass.edu.

[‡]Email: fjousse@scf.fundp.ac.be.

Outline

I. Introduction

II. Atomistic Dynamics in Zeolites

A. Basic Model and Forcefields

1. Zeolite Model
2. Guest-Zeolite Forcefields

B. Equilibrium Molecular Dynamics

1. Ensembles and Parameters
2. Data Analyses
3. Recent Applications

C. Reactive Flux Molecular Dynamics and Transition-State Theory

1. Rare Event Theory
2. Recent Applications

III. Lattice Dynamics in Zeolites

A. Fundamental Assumptions

B. Kinetic Monte Carlo

1. Algorithms and Ensembles
2. Data Analyses
3. Models of Finite Loading
4. Recent Applications

C. Mean Field and Continuum Theories

1. Finite Loading Effects
2. Fickian vs. Maxwell-Stefan Theory
3. Recent Applications

IV. Concluding Remarks

V. Acknowledgments

I. INTRODUCTION

Zeolites are nanoporous crystalline aluminosilicates with a rich variety of interesting properties and industrial applications.^{1–3} With over 100 zeolite framework topologies^{4–6} synthetically available—each with its own range of compositions—zeolites offer size-, shape- and electrostatically-selective adsorption,⁷ diffusion^{8,9} and reaction⁷ up to remarkably high temperatures. The impressive selectivities produced by these materials result from strong guest-zeolite interactions; however, these same interactions can severely retard the eventual permeation of desired products from zeolites. This has led to growing interest in modeling the transport of molecules in zeolites, to seek an optimal balance between high selectivity and high flux by identifying the fundamental interaction parameters that determine these key properties. In this review, we describe recent efforts using atomistic methods and lattice models to simulate the dynamics of sorbed molecules in zeolites.

Practical applications of zeolites are typically run under steady-state conditions, making the relevant transport coefficient the Fickian diffusivity or other related permeability coefficient. However, modeling such steady-state transport through zeolites with atomistic models is challenging, prompting many researchers instead to simulate self diffusion, which is the stochastic motion of tagged particles at equilibrium. Although self diffusivities for molecular liquids over a wide temperature range typically fall in the range of 10^{-9} – 10^{-8} $\text{m}^2 \text{s}^{-1}$, self diffusivities for molecules in zeolites cover a much larger range, from 10^{-19} $\text{m}^2 \text{s}^{-1}$ for benzene in Ca-Y¹⁰ to 10^{-8} $\text{m}^2 \text{s}^{-1}$ for methane in silicalite-1.¹¹ Such a wide range offers the possibility that diffusion in zeolites, probed by both experiment and simulation, can provide an important characterization tool complementary to diffraction, NMR, IR, etc., because diffusive trajectories of molecules in zeolites sample all relevant regions of the guest-zeolite potential energy surface. Below we assess the accuracy with which modern dynamics simulations can predict self diffusivities of molecules in zeolites, and discuss the insights gained from such simulations regarding guest-zeolite structure.

The wide range of diffusional time scales encountered by molecules in zeolites presents unique challenges to the modeler, requiring that various simulation tools, each with its own range of applicability, be brought to bear on modeling dynamics in zeolites. In particular, when transport is relatively rapid, the molecular dynamics technique can be used to simulate both the temperature and loading dependencies of self diffusion.^{12,13} On the other hand, when molecular motion is relatively slow because free energy barriers separating sorption sites are large compared to thermal energies, transition-state theory and related methods must be used to simulate the temperature dependence of site-to-site jump rate constants. In this regime, kinetic Monte Carlo and mean field theory can then be used to model the loading dependence of activated diffusion in zeolites.^{14,15} In this review we describe the techniques and applications of these methods, focusing on how the interplay between guest-zeolite adhesion and guest-guest cohesion controls diffusion in zeolites.

The goal of most diffusion simulations is to predict the temperature and loading dependencies of self diffusion in various zeolites with different framework topologies, and over a range of Si:Al ratios. One generally expects self diffusivities to exhibit an Arrhenius temperature dependence, with the apparent activation energy controlled by migration through bottlenecks such as narrow channels or cage windows. In addition, one typically observes that self diffusivities decrease linearly with loading as site blocking decreases the number of

successful jump attempts. While these ideas provide useful rules of thumb, we see below that guest-zeolite systems provide many fascinating examples that break these long-honored rules. We also find below that with modern tools of theory and simulation, researchers have produced remarkably useful insights and accurate predictions regarding the dynamics of sorbed molecules in zeolites.

II. ATOMISTIC DYNAMICS IN ZEOLITES

The goals of simulating molecular dynamics in zeolites with atomistic detail are two-fold: to predict the transport coefficients of adsorbed molecules, and to elucidate the mechanisms of intracrystalline diffusion. Below we discuss the basic assumptions and forcefields underlying such simulations, as well as the dynamics methods used to model both rapid and activated motion through zeolites.

A. Basic Model and Forcefields

1. Zeolite Model

Ordered Models. Modeling the dynamics of sorbates in zeolites requires an adequate representation of the zeolite sorbent. Zeolites are crystalline materials, which simplifies tremendously the modeler’s task as compared to the task of modeling amorphous or disordered microporous materials such as silica gels or activated carbons. Zeolite framework structures are well-known from many crystallographic studies and easily accessible from reference material such as Meier and Olson’s Atlas of Zeolite Structure Types,⁴ commercial⁵ or internet databases.⁶ Moreover, the typical size of a zeolite crystallite is 1 to 100 μm , that is, much larger than the length scale probed by atomistic molecular dynamics simulations. Size effects therefore can often be neglected except for single-file systems,¹⁶ and an adequate modeling of the sorbent is obtained with only a few unit cells included in the simulation cell, with periodic boundary conditions to represent the crystallite’s extent.

However, a zeolite structure presents some heterogeneities at the atomistic scale: the arrangement of Si and Al atoms in the structure (or Al and P for AlPO_4 ’s) usually does not present any long-ranged ordering; and in the general case, extra-framework cations also occupy crystallographic positions without full occupancy or long-range ordering. The simplest way to tackle this problem is to ignore it completely; indeed, a good 80% of all molecular dynamics (MD) studies of guest dynamics in zeolites published since 1997 concern aluminum-free, cation-free, defect-free all-silica zeolite analogs rather than zeolites. These structures sometimes exist, such as silicalite-1, silicalite-2 and ZDDAY, the respective analogs of ZSM-5 (structure MFI), ZSM-11 (structure MEL) and Na-Y (structure FAU). However, the siliceous analogs sometimes do not exist but in the modeler’s view, such as LTL, the analog of the cation-containing zeolite L. Nevertheless, these models can be very useful for studying the influence of zeolite structure or topology on an adsorbate’s dynamics, irrespective of the cations,¹⁷ or to determine exactly, by comparison, the cations’ influence.^{18,19} Furthermore, some zeolites of industrial interest such as ZSM-5 present high Si:Al ratios, so that their protonated forms have very few protons per unit cell. Heink *et al.* have shown, for example,

that the Si:Al ratio of ZSM-5 has very little influence on hydrocarbon diffusivity.²⁰ In these cases, it is safe to assume that studying diffusion in a completely siliceous zeolite analog will display most characteristics of the diffusion in the protonated form. This assumption simplifies several factors of the simulation and of the subsequent analysis: fewer parameters for the guest-zeolite interaction potential are needed, the system does not present any heterogeneity, and electrostatic interactions can be neglected when using adequate van der Waals interaction parameters, therefore decreasing the computational cost of a force evaluation.

Charge Distributions. There are many cases where such a simplified representation is inadequate: in particular, exchangeable cations create an intense local electric field (amounting to 3 V/Å next to a Ca²⁺ cation in Na-A, according to induced IR measurements)²¹ so that, unless the cation is inaccessible to the sorbate, one cannot neglect its Coulombic interaction with an adsorbed molecule. The number of cations in the frame depends on the Si:Al ratio: each Al atom brings one negative charge to be compensated by the adequate number of mono or multivalent cations. Hence the Si:Al ratio strongly influences the adsorptive properties of zeolites, so much that a change in the amount of Al brings a change in nomenclature: for example, FAU-type zeolites are denoted zeolite X for Si:Al < 1.5 and zeolite Y for a Si:Al > 1.5. Many groups have investigated the distribution of Al and Si atoms in zeolites, to determine whether there is any local arrangement of these atoms.^{22–27} Since X-ray crystallography does not distinguish Si from Al, this is necessarily determined from indirect techniques such as Si or Al NMR. Löwenstein’s rule forbids any Al–O–Al bonds, which brings perfect ordering for Si:Al=1, such as in Na-A. In most other cases, no local ordering has been found in the studies mentioned above. An exception is zeolite EMT, where rich Si and Al phases have been found from crystallographic measurements, when synthesized using crown ethers as templates.²⁸ In zeolite L, aluminum atoms preferentially occupy T₁ rather than T₂ sites, as found out by neutron crystallography.²⁹

In the absence of local ordering, a common modeling procedure involves neglecting the local inhomogeneity of the Si:Al distribution, and replacing all Al or Si by an average tetrahedral atom T, which is exactly what is observed crystallographically. The Si:Al ratio then is reflected by the average charge of this T atom, the charges on framework oxygen atoms, and by the number of charge compensating cations. This T-site model has been used in many recent modeling studies, and performs very well for reproducing adsorptive properties of zeolites.^{30,31} Indeed, few studies of guest adsorption in zeolites consider explicit Al and Si atoms.^{32–34}

The most important inhomogeneity inside cation-containing zeolites comes from the cation distribution. Indeed, except for very special values of the Si:Al ratio, the possible cation sites are not completely or symmetrically filled, and crystallographic measurements only give average occupancies. A common procedure is to use a simplified model, with just the right Si:Al ratio that allows complete occupancy of the most probable cation sites and no cations in other sites. This has been used, e.g., by Santikary and Yashonath in their modeling of diffusion in zeolite Na-A: instead of Si:Al=1, they used a model Na-A with Si:Al=2, thus allowing complete occupancy of cation site I, which gives cubic symmetry of the framework.³⁵ Similarly, Auerbach and coworkers used a model zeolite Na-Y with Si:Al=2 in a series of studies on benzene diffusion, so that the model would contain just the right number of Na cations to fill sites I’ and II, thereby giving tetrahedral symmetry.^{18,36,37} In studying Na-X, which typically involves Si:Al=1.2, they used Si:Al=1 so that Na(III) would

also be filled.¹⁸ This type of procedure is generally used to level off inhomogeneities that complicate the analysis.

It is instructive to observe the effect of the Si:Al ratio of FAU-type zeolites on the behavior of benzene diffusion, as determined from modeling.^{18,36,38} For very high Si:Al ratios no cations are accessible to sorbed benzene, which only feels a weak interaction with the framework, and hence diffuses over shallow energetic barriers. These reach only 10 kJ mol⁻¹ between the supercage sites and window sites, where benzene adsorbs in the plane of the 12 T-atom ring (12R) window separating two adjacent supercages.³⁸ As the Si:Al ratio decreases toward Na-Y, cation sites II begin to fill in as indicated in figure 1. These Na(II) cations at tetrahedral supercage positions create strong local adsorption sites for benzene (the S_{II} site), while the window site remains unchanged. As a consequence, the energetic barrier to diffusion increases to *ca.* 40 kJ mol⁻¹.³⁶ The spread in measured activation energies for benzene in Na-Y shown in figure 1 reflects both intracage and cage-to-cage dynamics,³⁹ because both NMR relaxation data (intracage) and diffusion data (cage-to-cage) are shown. When the Si:Al ratio further decreases toward Na-X, the windows are occupied by strongly adsorbing site III cations. As a consequence, the window site is replaced by a strong S_{III} site where benzene is facially coordinated to the site III cation, so that transport is controlled by smaller energy barriers reaching only about 15 kJ mol⁻¹.¹⁸ Figure 1 (top and middle) schematically presents this behavior, while on the bottom part we compare the expected behavior of the activation energy (full line) as a function of Si:Al ratio to the available experimental observations (points). The correlation between simulation and experiments is qualitatively reasonable considering the spread of experimental data. Figure 1 shows the success of using a particular Si:Al ratio to simplify the computation, and furthermore shows that adding cations in the structure does not necessarily result in an increase of the diffusion activation energy.

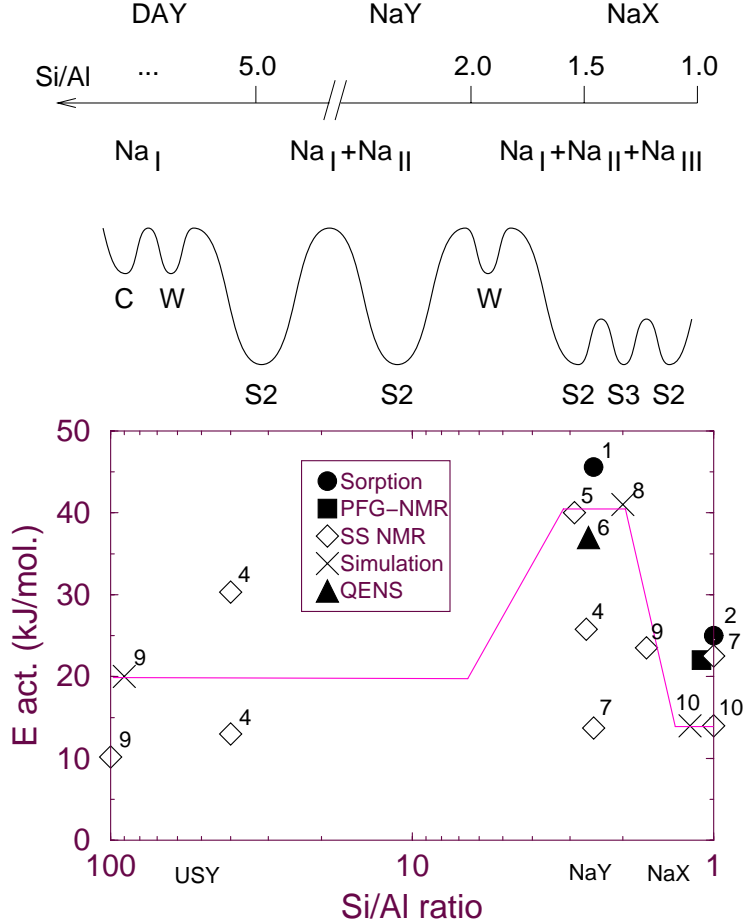


Figure 1. Activation energies of benzene diffusion in FAU-type zeolites. The top part shows Si:Al ratios of FAU-type zeolites, with the corresponding occupied cation sites. The middle part represents schematic benzene adsorption sites, and the energy barriers between them arising from different cation distributions. C is a benzene supercage site far from a cation, W is a benzene window site far from a cation, S₂ is a cage site close to an S_{II} cation, S₃ is a window site close to an S_{III} cation. The bottom part gives diffusion activation energies for various Si:Al ratios. The solid line shows the overall trend from simulations, symbols are particular experiment or simulation results: 1 Forni *et al.*,⁴⁰ 2. Bülow *et al.*,⁴¹ 3. Lorenz *et al.*,⁴² 4. Sousa-Gonçalves *et al.*,⁴³ 5. Isfort *et al.*,⁴⁴ 6. Jobic *et al.*,⁴⁵ 7. Burmeister *et al.*,⁴⁶ 8. Auerbach *et al.*,³⁶ 9. Bull *et al.*⁴⁷ and 10. Auerbach *et al.*¹⁸

Despite the success of treating disordered charge distributions as being ordered, Chen *et al.* have suggested that electrostatic traps created by disordered Al and cation distributions can significantly diminish self diffusivities from their values for corresponding ordered systems.⁴⁸ In addition, when modeling the dynamics of exchangeable cations⁴⁹ or molecules in acidic zeolites,³⁴ it may be important to develop more sophisticated zeolite models which completely sample Al and Si heterogeneity, as well as the possible cation distributions. For example, Newsam and coworkers proposed an iterative strategy allowing the placement of exchangeable cations inside a negatively charged framework,⁵⁰ implemented within MSI's Cerius2 modeling environment. In addition, we have constructed a model zeolite H-Y (Si:Al=2.43) by randomly placing aluminum atoms in the frame, and distributing protons

using the following three rules: (i) protons are linked to an oxygen close to an Al atom; (ii) no two hydroxyl groups can be linked to the same silicon atom; (iii) no proton can be closer than 4.0 Å from another.³⁴ Although these rules do not completely determine the proton positions, we found that several different proton distributions were broadly equivalent as far as sorption of benzene is concerned. It is clear from the above examples that the real issue in modeling the dynamics of sorbed molecules in zeolites comes from the interaction potentials, also known as forcefields when computed from empirical functional forms. Before discussing these forcefields in the context of dynamics, however, we examine a hot topic among scientist in the field: whether framework vibrations influence the dynamics of guest molecules in zeolites.

Framework Flexibility. This question has long remained an open one, but many recent studies have made systematic comparisons between fixed and flexible lattice simulations, based on several examples: methane and light hydrocarbons in silicalite-1,^{51–55} methane in cation-free LTA,⁵⁶ Lennard-Jones adsorbates in Na-A³⁵ and in Na-Y,⁵⁷ benzene and propylene in MCM-22,⁵⁸ benzene in Na-Y,^{59–61} and methane in AlPO₄-5.⁶² In cation-free zeolites, these recent studies have found that diffusivities are virtually unchanged when including lattice vibrations. Fritzsche *et al.*⁵⁶ explained earlier discrepancies on methane in cation-free LTA zeolite by pointing out that inappropriate comparisons were made between rigid and flexible framework studies. In particular, the rigid studies used crystallographic coordinates for the framework atoms, while the forcefield used to represent the framework vibrations gave a larger mean window size than that in the rigid case, thereby resulting in larger diffusivities in the flexible framework. By comparing with a model rigid LTA minimized using the same forcefield, they found almost no influence on the diffusion coefficient. Similarly, Demontis *et al.* have studied the diffusion of methane in silicalite-1, with rigid and flexible frameworks.⁵³ They conclude that the framework vibrations do not influence the diffusion coefficient, although they affect local dynamical properties such as the damping of the velocity autocorrelation function. Following these findings, numerous recent diffusion studies of guest hydrocarbons or Lennard-Jones adsorbates in cation-free zeolites keep the framework rigid.^{17,63–71}

There are, however, some counter-examples in cation-free zeolites. In a recent MD study of benzene and propylene in MCM-22 zeolite, Sastre, Catlow and Corma found differences between the diffusion coefficients calculated in the rigid and flexible framework cases.⁵⁸ Bouy-ermaouen and Bellemans also observe notable differences for i-butane diffusion in silicalite-1.⁵⁵ Snurr, Bell and Theodorou used TST to calculate benzene jump rates in a rigid model of silicalite-1,⁷² finding diffusivities that are one to two orders of magnitude smaller than experimental values. Forester and Smith subsequently applied TST to benzene in flexible silicalite-1,⁷³ finding essentially quantitative agreement with experiment, thus demonstrating the importance of including framework flexibility when modeling tight-fitting guest-zeolite systems.

Strong framework flexibility effects might also be expected for molecules in cation-containing zeolites, where cation vibrations strongly couple to the adsorbate’s motions, and where diffusion is mostly an activated process. However, where a comparison between flexible and fixed framework calculations has been performed, surprisingly little influence has been found. This has been shown by Santikary and Yashonath for the diffusion of Lennard-Jones adsorbates of varying size in Na-A. They found a notable difference on the adsorbate

density distribution and external frequencies, but not on diffusion coefficients.³⁵ Mosell *et al.* found that the potential of mean force for the diffusion of benzene in Na-Y remains essentially unchanged when framework vibrations are included.⁵⁹ Jousse *et al.* also found that the site-to-site jump probabilities for benzene in Na-Y do not change when including framework flexibility, in spite of very strong coupling between benzene’s external vibrations and the Na(II) cation.⁶¹ The reasons behind this behavior remain unclear, and it is also doubtful whether these findings can be extended to other systems. Nevertheless, the direct examination of the influence of zeolite vibrations on guest dynamics suggests the following: a strong influence on local static and dynamical properties of the guest, such as low-frequency spectra, correlation functions and density distributions; a strong influence on the activated diffusion of tight-fitting guest-zeolite systems; but a small influence on diffusion of smaller molecules such as unbranched alkanes.

The preceding discussion on framework flexibility, and its impact on molecular dynamics, has the merit of pointing out the two important aspects for modeling zeolites: structural and dynamical. On the structural side, the zeolite cation distribution, channel diameters and window sizes must be well represented. On the dynamical side, for tight-fitting host-guest systems, the framework vibrations must allow for an accurate treatment of the activation energy for molecular jumps through flexing channels and/or windows. Existing zeolite framework forcefields are numerous and take many different forms, but they are generally designed for only one of these purposes. It is beyond the scope of this article to review zeolite framework forcefields;¹³ we simply wish to emphasize that one should be very cautious in choosing the appropriate forcefield designed for the properties to be studied.

2. Guest-Zeolite Forcefields

The guest-framework forcefield is the most important ingredient for atomistic dynamical models of sorbed molecules in zeolites. Forcefields for guest-zeolite interactions are at least as diverse as those for the zeolite framework: even more so, in fact, as most studies of guest molecules involve a re-parameterization of potential energy functions to reproduce some typical thermodynamical property of the system, such as adsorption energies or adsorption isotherms. Since forcefields are but an analytical approximation of the real potential energy surface, it is essential that the underlying physics is correctly captured by the analytical form. Every researcher working in the field has a different opinion on what the correct form should be; therefore the following discussion must necessarily remain subjective, and we refer the reader to the original articles to sample different opinions.

Physical contributions to the interaction energy between host and guest are numerous: most important are the short range dispersive and repulsive interactions, and the electrostatic multipolar and inductive interactions. Nicholson and coworkers developed precise potentials for the adsorption of rare gases in silicalite-1, including high-order dispersive terms,⁷⁴ and have shown that all terms contribute significantly to the potential energy surface,⁷⁵ the largest contributions coming from the two and three body dispersion terms. Cohen de Lara and coworkers developed and applied a potential function including inductive terms for the adsorption of diatomic homonuclear molecules in A-type zeolites.^{76,77} Here also the induction term makes a large contribution to the total interaction energy. A general

forcefield would have to account for all these different contributions, but most forcefields completely neglect these terms for the sake of simplicity. Simplified expressions include only a dispersive-repulsive short-ranged potential, often represented by a Lennard Jones 6-12 or a Buckingham 6-exp. potential, possibly combined with electrostatic interactions between partial charges on the zeolite and guest atoms, according to:

$$U_{ZG} = \sum_I \sum_j \left\{ \frac{q_I q_j}{r_{Ij}} - \frac{A_{Ij}}{r_{Ij}^6} + \frac{B_{Ij}}{r_{Ij}^{12}} \right\}. \quad (2.1)$$

In general, the parameters A and B are determined by some type of combination rule from “atomic” parameters, and adjusted to reproduce equilibrium properties such as adsorption energies or adsorption isotherms. It is unlikely, however, that such a potential is transferable between different guest molecules or zeolite structures. As such, the first step of any study utilizing such a simple forcefield on a new type of host or guest should be the computation of some reference experimental data, such as the heat of adsorption, and eventually the re-parametrization of forcefield terms. Indeed, general purpose forcefields such as CVFF do not give generally adequate results for adsorption in zeolites.^{78,79}

The simplification of the forcefield terms can proceed further: in all-silica zeolite analogs with small channels, the electric field does not vary much across the channel and as a consequence the Coulombic term in equation 2.1 can often be neglected. This is of course not true for cation-containing zeolites, where the cations create an intense and local electric field that generally gives rise to strong adsorption sites. Since evaluating electrostatic energies is so computationally demanding, neglecting such terms allows for much longer dynamics simulations. Another common simplification is to represent CH_2 and CH_3 groups in saturated hydrocarbons as united atoms with their own effective potentials. These are very frequently used to model hydrocarbons in all-silica zeolites.^{56,64,65,67,80} There is, however, active debate in the literature whether such a simplified model can account for enough properties of adsorbed hydrocarbons.^{81–83}

The standard method for evaluating Coulombic energies in guest zeolite systems is the Ewald method,^{84,85} which scales as $n \ln n$ with increasing number of atoms n . In 1987 Greengard and Rokhlin⁸⁶ presented the alternative “Fast Multipole Method” (FMM) which only scales as n , and therefore offers the possibility of simulating larger systems. In general FMM only competes with the Ewald method for systems with many thousand atoms,⁸⁷ and therefore is of little use in zeolitic systems where the simulation cell can usually be reduced to a few hundreds or a few thousand atoms. However, in the special case where the zeolite lattice is kept rigid, most of the terms in FMM can be precomputed and stored; in this case we have shown that FMM becomes faster than Ewald summation for benzene in Na-Y.³⁷

This section would not be complete without mentioning the possibility of performing atomistic simulations in zeolites without forcefields,⁸⁸ using *ab initio* molecular dynamics (AIMD).^{89,90} Following the original work of Car and Parrinello, most such studies use density functional theory and plane wave basis sets.⁹¹ This technique has been applied recently to adsorbate dynamics in zeolites.^{92–100} Beside the obvious interest of being free of systematic errors due to the forcefield, this technique also allows the direct study of zeolite catalytic activity.^{92–94} However, AIMD remains so time consuming that a dynamical simulation of a zeolite unit cell with an adsorbed guest only reaches a few ps at most. This time scale is too

short to follow diffusion in zeolites, so that current simulations are mostly limited to studying vibrational behavior.^{92–97} Similarly, catalytic activity is limited to reactions with activation energies on the order of thermal energies.^{92,94,98} However, the potential of AIMD to simulate transport coefficients has been demonstrated for simpler systems,^{101,102} and will likely extend to guest-zeolite systems in the near future as computers and algorithms improve.

B. Equilibrium Molecular Dynamics

Since the first application of equilibrium MD to guest molecules adsorbed in zeolites in 1986,¹⁰³ the subject has attracted growing interest.^{13,15} Indeed, MD simulations provide an invaluable tool for studying the dynamical behavior of adsorbed molecules over times ranging from ps to ns, thus correlating atomistic interactions to experiments that probe molecular dynamics, including: solid state NMR, pulsed field gradient NMR (PFG NMR), inelastic neutron spectroscopy (INS), quasi-elastic neutron scattering (QENS), IR and Raman spectroscopy.

MD of guest molecules in zeolites is conceptually no different from MD simulations of any other nanosized system. Classical MD involves numerically integrating classical equations of motion for a many-body system. For example, when using Cartesian coordinates, one can integrate Newton’s second law: $\mathbf{F}_i = m_i \mathbf{a}_i$ where m_i is the mass of the i^{th} particle, $\mathbf{a}_i = d^2 \mathbf{r}_i / dt^2$ is its acceleration, and $\mathbf{F}_i = -\nabla_{\mathbf{r}_i} V$ is the force on particle i . The crucial inputs to MD are the initial positions and velocities of all particles, as well as the system potential energy function $V(\mathbf{r}_1, \mathbf{r}_2, \dots, \mathbf{r}_n)$. The output of MD is the dynamical trajectory $[\mathbf{r}_i(t), \mathbf{v}_i(t)]$ for each particle. All modern techniques arising in the field can be applied to the simulation of zeolites, including multiple time scale techniques, thermostats and constraints. The interested reader is referred to textbooks on the method,^{85,104} and to modern reviews.^{105,106} In this section we shall describe only those aspects of MD that are especially pertinent to molecules in zeolites. A comprehensive review on MD of guest molecules in zeolites was published in 1997 by Demontis and Suffritti.¹³ Because the review by Demontis and Suffritti discusses virtually all applications of the method up to 1996, we will limit our examples to the most recent MD studies.

1. Parameters and Ensembles

Parameters. Equilibrium MD is generally composed of two stages: an equilibration run, allowing the system to relax to equilibrium, and a production run, during which data are gathered for later analysis. Typically the equilibration is initiated from some initial configuration of the adsorbate (randomly chosen or from an energy minimum) with initial velocities assigned from a Maxwell-Boltzmann distribution. The duration required to reach equilibrium depends on the relaxation time of the system: in general larger systems presenting strong correlations, e.g. at high loading, require much longer equilibration times than do smaller systems. For example, Gergidis and Theodorou have used equilibration times ranging from 0.5 to 2 ns for low to high loading of mixtures of methane and n-butane in silicalite-1.⁷⁰ Other groups, however, used much shorter equilibration runs: Clark *et al.*⁶⁴ or Schuring *et al.*⁶⁷ used equilibration runs of 50 to 125 ps for long alkanes in silicalite-1,

while Sastre and coworkers, who used a much more complex and computationally demanding forcefield with a flexible framework, limited the equilibration runs to 25 ps.^{58,82,83} Schrimpf *et al.* have directly studied the relaxation of adsorbed xenon and one-center methane in a model Na-Y, using non-equilibrium molecular dynamics.⁵⁷ We have recently investigated the relaxation of benzene in Na-Y at infinite dilution.⁶¹ Both these studies show that relaxation is influenced by framework vibrations, lateral interactions between guest molecules and coupling with the internal degrees of freedom. However, in all cases relaxation remains quite fast, decaying exponentially with a time constant of *ca.* 5 ps for benzene at 100 K,⁶¹ 11 ps for methane and 25 ps for xenon at 300 K. The equilibration run is generally performed in the canonical ensemble to achieve a desired temperature;¹³ since the dynamics is not monitored, any method of temperature control can be used.

Equilibrium MD calculations are mostly performed to generate trajectories for studying adsorbate self diffusion. Special care should be taken to ensure that the trajectories are indeed long enough to compute a statistically converged self-diffusion coefficient. We estimate that the current limiting diffusivity, below which adsorbate motion is too slow for equilibrium MD, is around $D_{\min} \approx 5 \times 10^{-10} \text{ m}^2 \text{ s}^{-1}$, obtained by supposing that a molecule travels over 10 unit cells of 10 Å during a 20 ns MD run. This value of D_{\min} is higher than most measured diffusivities in cation-containing zeolites,⁸ explaining why so many MD studies focus on hydrocarbons in all-silica zeolite analogs. Even then, the simplifications discussed above are required in order to perform MD runs of several ns in a manageable time: simple Lennard-Jones forcefields on united atom interaction centers without Coulombic interactions, bond constraints on C–C bonds allowing for longer time steps, and the use of fixed frameworks.

Ensembles. A flexible zeolite framework typically provides an excellent thermostat for the sorbate molecules. The framework temperature exhibits minimal variations around its average value, while the sorbate energy fluctuates in a way consistent with the canonical ensemble. This is valid either for a microcanonical (*NVE*) ensemble run, or a canonical (*NVT*) ensemble run involving mild coupling to an external thermostat. We caution that coupling the system too strongly to an external bath will almost surely contaminate the actual sorbate dynamics.

The problem is clearly more complex when the zeolite framework is kept rigid. Ideally, one should run the dynamics in the canonical ensemble, with just the right coupling constant to reproduce the fluctuations arising from a flexible framework. When these fluctuations are unknown, however, it is not obvious whether a canonical or microcanonical run is better. In the *NVE* ensemble, the sorbate does not exchange energy with a bath, which may lead to incorrect energy statistics. This is particularly true at low loading, but may remain true for higher loadings as well. Indeed, in a direct study of the kinetic energy relaxation of Lennard-Jones particles in Na-Y, Schrimpf *et al.* found that the thermalization due to interactions with the framework is considerably faster than the thermalization due to mutual interactions between the adsorbates.⁵⁷ Therefore, it is probably better to run the dynamics in the *NVT* ensemble, with sufficiently weak coupling to an external thermostat to leave the dynamics uncontaminated. On the other hand, we have shown that for non-rigid benzene in Na-Y, there is very rapid energy redistribution from translational kinetic energy into benzene’s internal vibrational degrees of freedom,⁶¹ which proceeds on a time scale comparable to the thermalization due to interactions with the flexible frame. This suggests that for sufficiently large, flexible guest molecules, the transport behavior can be adequately modeled in the

NVE ensemble even at infinite dilution.

Although this section focuses on equilibrium MD, we note growing interest in performing non-equilibrium MD (NEMD) simulations on guest zeolites systems. As an aside, we note that MD experts would classify thermostatted MD, and any non-Newtonian MD for that matter, as NEMD.^{107,108} We shall be much more restrictive and limit the non-equilibrium behavior to studies involving an explicit gradient along the system, resulting in a net flow of particles. This is especially interesting in zeolite science, because most applications of zeolites are run under non-equilibrium conditions, and also because of recent progress in the synthesis of continuous zeolite membranes.^{109,110} In this case we seek the Fickian or “transport” diffusivity, defined by Fick’s law: $J = -D\nabla\theta$, where J is the net particle flux, D is the transport diffusivity, and $\nabla\theta$ is the local concentration gradient. These concepts are discussed more thoroughly in section III C 2; here we only wish to discuss ensembles relevant to this NEMD.

A seminal study was reported in 1993 by Maginn, Bell and Theodorou, reporting NEMD calculations of methane transport diffusion through silicalite-1.¹¹¹ They applied gradient relaxation MD as well as color field MD, simulating the equilibration of a macroscopic concentration gradient and the steady-state flow driven by an external field, respectively. They found that the color field MD technique provides a more reliable method for simulating the linear response regime. Since then, NEMD methods in the grand canonical ensemble have been reported. Of particular interest is the “dual volume control grand canonical molecular dynamics” (DVC-GCMD) method, presented by Heffelfinger and van Swol.¹¹² In this approach the system is divided in three parts, a central and two boundary regions. In the central region, regular molecular dynamics is performed, while in the boundary regions creation and annihilation of molecules are allowed to equilibrate the system with a given chemical potential, following the grand canonical Monte Carlo procedure. This or similar methods have been applied to the simulation of fluid-like behavior in slit pores of very small dimensions (down to a few σ).^{113–118} To our knowledge, however, no such simulation has been applied to Fickian diffusion in structured zeolite pores, presumably because it would depend on details of zeolite crystallite surface structure. Nonetheless, this is likely to be an important area of future research.

2. Data Analyses

Most equilibrium MD studies aim to determine the self-diffusion coefficient of the adsorbed molecules within the zeolite pores. The self-diffusivity is defined by Einstein’s relation:

$$D_s = \lim_{t \rightarrow \infty} \frac{1}{6t} \langle |\mathbf{r}(t) - \mathbf{r}(0)|^2 \rangle, \quad (2.2)$$

that is, it is proportional to the long-time limiting slope of the mean-square displacement (MSD). This expression assumes that for $t \rightarrow \infty$, the guest diffusion becomes Fickian, so that the MSD becomes linear with t . This is valid whenever the motions of the adsorbates are not too strongly correlated. An extreme case of correlation between molecular motions is single-file diffusion, where molecules diffusing in unidirectional narrow channels must necessarily

diffuse all together or not at all. This type of behavior has recently been experimentally observed for the diffusion of tetrafluoromethane in $\text{AlPO}_4\text{-5}$.^{119,120} In that case, correlations extend to infinity and the behavior of the MSD as a function of t at long time depends on the boundaries of the model:¹²¹ linear for open boundaries, plateau for closed boundaries and \sqrt{t} for an infinite system.

Although MD becomes inefficient for modeling activated diffusion, MD can provide useful information about such transport when barriers are comparable to $k_B T$. In this case, MD can be used to define a coarse-grained model of diffusion.^{122,123} This coarse-graining requires two inputs: the lattice of sites on which diffusion takes place, and the kinetic law governing the motions between those sites. The analysis of MD trajectories as a jump diffusion process allows one to determine the adsorption sites, by monitoring the positions of maximum probability of the adsorbate during the dynamics,¹²³ as well as the details of the kinetic law. It has generally been found that residence time distributions follow a simple exponential dependence, characteristic of random site-to-site jumps. In figure 2, we present such a residence time distribution for the example of benzene diffusing in zeolite LTL, clearly showing this signature. These observations support the usual assumption of Poisson dynamics, central to many lattice models of guest diffusion in zeolites (see section III A). However, one often finds correlations between jumps that complicate the coarse-grained representation of diffusion.^{123–125}

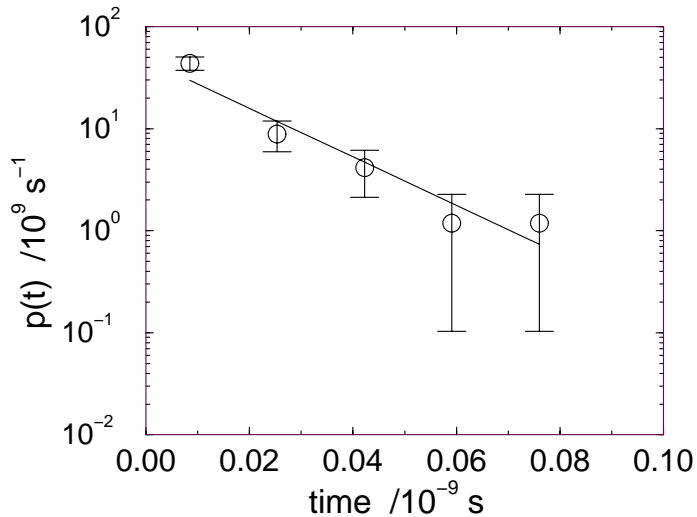


Figure 2. Cage residence time distribution of benzene in zeolite LTL showing agreement with Poisson statistics, computed from a 1 ns molecular dynamics simulation at 800 K with a single benzene molecule in the simulation cell.

Jump diffusion analyses of MD are particularly useful for comparing with quasi-elastic neutron scattering (QENS) experiments. QENS experiments measure the scattering function $F(\mathbf{Q}, \omega)$, which is the space-time Fourier transform of the van Hove correlation function:

$$G(\mathbf{r}, t) = \frac{1}{N} \sum_{i=1}^N \langle \delta(\mathbf{r} + \mathbf{r}_i(t) - \mathbf{r}_i(0)) \rangle. \quad (2.3)$$

For an adsorbate containing hydrogen atoms, the largest part of the incoherent scattering comes from these atoms.¹²⁶ A model of their microscopic motions is required to determine

the mobility of the adsorbed molecule.¹²⁷ MD simulations can be used to provide a direct analysis of the microscopic motions, and therefore to guide the interpretation of experiments. For example, Gaub *et al.* derived a simplified analytical formula for the van Hove correlation function of an adsorbate diffusing in a periodic zeolite structure.⁶³ Recently, Gergidis, Jobic and Theodorou analyzed QENS experiments of mixtures of methane and butane in silicalite-1 using a jump diffusion model, with the distribution of jumps extracted from their MD simulations.⁸⁰

When $k_B T$ is comparable to or greater than barriers between sites, the self-diffusion coefficient can also be determined from the velocity autocorrelation function, according to:

$$D_s = \frac{1}{3} \int_0^\infty dt \langle \mathbf{v}(t) \cdot \mathbf{v}(0) \rangle, \quad (2.4)$$

where $\mathbf{v}(t)$ indicates the instantaneous velocity of the adsorbate's center-of-mass. This equation shows that the self-diffusion coefficient is proportional to the zero-frequency component of the power spectrum $G(\omega)$ of the adsorbed molecule:

$$G(\omega) = \frac{1}{2\pi c} \int dt \frac{\langle \mathbf{v}(t) \cdot \mathbf{v}(0) \rangle}{\langle \mathbf{v}(0) \cdot \mathbf{v}(0) \rangle} e^{i\omega t}. \quad (2.5)$$

This spectrum, as well as spectra coming from other correlation functions, give particularly useful information about structure and dynamics, thereby providing additional ways to assess the validity of forcefields used in dynamics simulations.⁷⁹ The interested reader is referred to classical textbooks on MD simulations for more details on obtaining these spectra.^{85,104} Some recent applications include the computation of low-frequency IR and Raman spectra of cationic exchanged EMT zeolites by Bougeard *et al.*,¹²⁸ and our study of the external vibrations and rotations of benzene adsorbed in faujasite, with comparison to inelastic neutron scattering experiments.⁷⁹

3. Recent Applications

Dynamics of Hydrocarbons in Silicalite-1 and 10R Zeolites. Zeolite ZSM-5 is used in petroleum cracking, which explains the early interest in modeling the diffusion of alkanes in silicalite-1, the all-silica analog of ZSM-5.^{51-53,122,129-131} This early work has been reviewed by Demontis and Suffritti in 1997,¹³ and therefore we only wish to outline recent studies.

As pointed out earlier, the relatively rapid diffusivity of alkanes in the channels of all-silica zeolites, at room temperature or above, makes these systems perfect candidates for MD simulations. In general, very good agreement is found between MD self-diffusivities and those of microscopic types of experiments, such as PFG NMR or QENS. Figure 3 gives an example of this agreement, for methane and butane in silicalite-1 at 300 K (MD data slightly spread for clarity). This good agreement, in spite of the crudeness of the potentials used, shows that the diffusivity of light alkanes in silicalite-1 depends on the forcefield properly representing the host-guest steric interactions, i.e. on the size and topology of the pores. Recognizing this, many recent studies focus on comparing diffusion coefficients for different alkanes in many different zeolite topologies, in an effort to rationalize different observed catalytic behaviors. Jousse *et al.* studied the diffusion of butene isomers at infinite dilution in 10R zeolites

with various topologies: TON, MTT, MEL, MFI, FER and HEU. They observed in all cases except for the structure TON, that trans-2-butene diffuses more rapidly than all other isomers.¹³² Webb and Grest studied the diffusion of linear decanes and n-methylnonanes in seven 10R zeolites: AEL, EUO, FER, MEL, MFI, MTT and TON.¹⁷ For MEL, MTT and MFI, they observe that the self-diffusion coefficient decreases monotonically as the branch position is moved toward the center (and the isomer becomes bulkier), while for the four other structures, D_s presents a minimum for another branch position, suggesting that product shape selectivity might play some role in determining the zeolite selectivity. More recently, Webb *et al.* studied linear and branched alkanes in the range $n = 7 - 30$ in TON, EUO and MFI.⁶⁸ Again they observe lattice effects for branched molecules, where D_s presents a minimum as a function of branch position dependent upon the structure. They note also some “resonant diffusion effect” as a function of carbon number, noted earlier by Runnebaum and Maginn:¹³³ the diffusivity becomes a periodic function of carbon number, due to the preferential localization of molecules along one channel and their increased diffusion in this channel. Schuring *et al.* studied the diffusion of C_1 to C_{12} in MFI, MOR, FER and TON for different loadings.⁶⁷ They also find some indication of a resonant diffusion mechanism as a function of chain length. Their study also indicates that the diffusion of branched alkanes is significantly slower than that of their linear counterparts, but only for structures with small pores where there is a tight fit between the adsorbates and the pores.

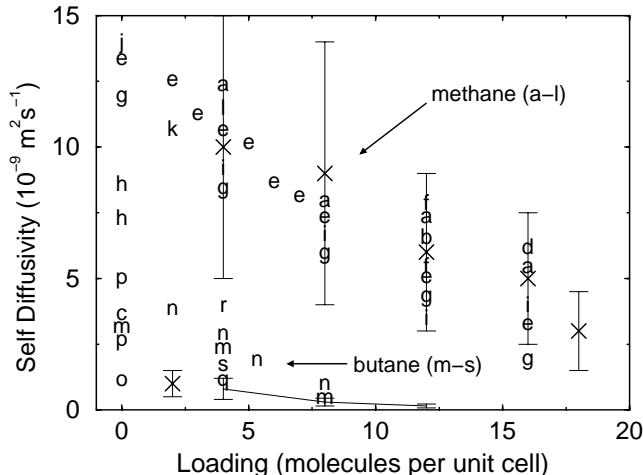


Figure 3. Self-diffusion isotherms of methane and butane in silicalite-1 at 300K, from PFG NMR, QENS and MD simulations, showing good agreement with the $(1 - \theta)$ loading dependence predicted by mean field theory. Crosses are NMR data from Caro *et al.*¹¹ for methane and Heink *et al.*²⁰ for butane, while the star shows QENS butane data from Jovic *et al.*¹³⁴ In all cases, error bars represent an estimated 50% uncertainty. Letters are MD results (slightly spread for clarity): a-l for methane and m-s for butane, from the following references: (a) June *et al.*,¹²⁹ (b) Demontis *et al.*,⁵¹ (c) Catlow *et al.*,⁵² (e) Goodbody *et al.*,¹³¹ (f) Demontis *et al.*,⁵³ (g) Nicholas *et al.*,¹³⁵ (h) Smirnov,⁵⁴ (i) Jost *et al.*,⁷¹ (j) Ermoshin and Engel,¹³⁶ (k) Schuring *et al.*,⁶⁷ (l) Gergidis and Theodorou,⁷⁰ (m) June *et al.*,¹²² (n) Hernández and Catlow,¹³⁷ (o) Maginn *et al.*,¹³⁸ (p) Bouyermaouen and Bellemans,⁵⁵ (q) Goodbody *et al.*,¹³¹ (r) Gergidis and Theodorou⁷⁰ and (s) Schuring *et al.*⁶⁷

Another current direction of research concerns the diffusion of mixtures of adsorbates. Although the currently preferred atomistic simulation method applied to the adsorption of mixtures is grand canonical Monte Carlo,^{139–143} MD simulations are also used to determine how the dynamics of one component affects the diffusion of the other.^{70,71,80,144} Sholl and Fichtorn investigated how a binary mixture of adsorbates diffuses in unidirectional pores,¹⁴⁴ finding a dual mode of diffusion for certain mixtures, wherein one component undergoes normal unidirectional diffusion while the other performs single-file diffusion. Jost *et al.* studied the diffusion of mixtures of methane and xenon in silicalite-1.⁷¹ They find that the diffusivity of methane decreases strongly as the loading of Xe increases, while the diffusivity of Xe is nearly independent of the loading of methane, which they attribute to the larger mass and heat of adsorption of Xe. On the other hand, Gergidis and Theodorou in their study of mixtures of methane and n-butane in silicalite-1,⁷⁰ found that the diffusivity of both molecules decreases monotonically with increasing loading of the other. Both groups report good agreement with PFG NMR⁷¹ and QENS experiments.⁸⁰

Single-File Diffusion. Single-file diffusion designates the particular collective motion of particles diffusing along a one-dimensional channel, and unable to pass each other. As already mentioned, in that case the long-time motions of the particles are completely correlated, so that the limit of the MSD depends on the boundaries of the system. Exact treatments using lattice models show that the MSD has three limiting dependencies with time:^{121,145} plateau for fixed boundaries, linear with t for periodic boundaries or open boundaries,¹⁶ and \sqrt{t} for infinite pore length. Experimental evidence for the existence of single-file behavior in unidimensional zeolites^{119,120,146,147} has prompted renewed interest in the subject during the last few years.^{16,65,66,148–152} In particular, several molecular dynamics simulations of more or less realistic single-file systems have been performed, in order to determine whether the single file \sqrt{t} regime is not an artifact of the simple lattice model on which it is based.^{65,66,69,150,151} Since the long-time motions of the particles in the MD simulations are necessarily correlated, great care must be taken to adequately consider the system boundaries. In particular, when using periodic boundary conditions, the system size along the channel axis must be sufficiently large to avoid the linear behavior due to the diffusion of the complete set of molecules.

Hahn and Kärger studied the diffusion of Lennard-Jones particles along a straight tube in three cases: (*i*) without external forces acting on the particles from the tube, (*ii*) with random forces, and (*iii*) with a periodic potential from the tube.¹⁵¹ They find for the no-force case that the MSD is proportional to t , whereas for random forces and a periodic potential it is proportional to \sqrt{t} , in agreement with the random walk model. Keffer *et al.* performed MD simulations of Lennard-Jones methane and ethane in an atomistic model of AlPO₄-5.¹⁵⁰ The methane molecules, which are able to pass each other, display unidirectional but otherwise normal diffusion with the MSD linear with t ; while ethane molecules, which have a smaller probability to pass each other, display single-file behavior with an MSD proportional to \sqrt{t} . For longer times, however, the nonzero probability to pass each other destroys the single-file behavior for ethane. Similar behavior was found by Tepper *et al.*⁶⁹ Sholl and coworkers investigated the diffusion of Lennard-Jones particles in a model AlPO₄-5,^{65,66,152} and found that diffusion along the pores can occur *via* concerted diffusion of weakly bound molecular clusters, composed of several adsorbates. These clusters can jump with much smaller activation energies than that of a single molecule. However, the MSD retains its

single-file \sqrt{t} signature because all the adsorbates in a file do not collapse to form a single supramolecular cluster.

These MD simulations of unidirectional and single-file systems confirm the lattice gas prediction, that the MSD is proportional to \sqrt{t} . They also show that whenever a certain crossing probability exists, this single-file behavior disappears at long times, to be replaced by normal diffusion. Similar “anomalous” diffusion regimes, with the MSD proportional to t at long times and to t^α with $\alpha < 1$ at short times, have also been found in other systems that do not satisfy the single-file criteria, such as n-butane in silicalite-1 at high loadings.⁷⁰ Therefore, one should be very careful to define exactly the time scale of interest when working with single-file or other highly correlated systems.

C. Reactive Flux Molecular Dynamics and Transition-State Theory

As discussed above in section II B 1, the smallest diffusivity that can be simulated by MD methods is well above most measured values in cation-containing zeolites,⁸ explaining why so many MD studies focus on hydrocarbons in all-silica zeolite analogs. This issue has been addressed by several groups within the last 10 years,¹⁵³ by applying reactive flux molecular dynamics^{154,155} (RFMD) and transition-state theory¹⁵⁶ (TST) to model the dynamics of rare events in zeolites. This subject has been reviewed very recently by Auerbach;¹⁵ as a result, we give below only a brief outline of the theory.

1. Rare Event Theory

The standard *ansatz* in TST is to replace the dynamically converged, net reactive flux from reactants to products with the instantaneous flux through the transition state dividing surface. TST is inspired by the fact that, although a dynamical rate calculation is rigorously independent of the surface through which fluxes are computed,¹⁵⁷ the duration of dynamics required to converge the net reactive flux is usually shortest when using the transition state dividing surface. The TST approximation can be formulated for gas phase or condensed phase systems,^{154,155,158} using classical or quantum mechanics.¹⁵⁹ The rate coefficient for the jump from site i to site j can be expressed classically as:^{154,155}

$$k_{i \rightarrow j} = k_{i \rightarrow j}^{\text{TST}} \times f_{ij}, \quad (2.6)$$

where $k_{i \rightarrow j}^{\text{TST}}$ is the TST rate constant, and f_{ij} is the dynamical correction factor also known as the classical transmission coefficient. The TST rate constant is given by:

$$k_{i \rightarrow j}^{\text{TST}} = \frac{1}{2} \left(\frac{2k_{\text{B}}T}{\pi m} \right)^{1/2} \frac{Q^\ddagger}{Q_i}, \quad (2.7)$$

where m is the reduced mass associated with the reaction coordinate, Q^\ddagger is the configurational partition function on the dividing surface and Q_i is the configurational partition function in the reactant state i . The last expression can be evaluated without recourse to dynamics, either by Monte Carlo simulation¹⁶⁰ or in the harmonic approximation by normal

mode analysis.¹⁶¹ The dynamical correction factor is usually evaluated from short molecular dynamics simulations originating on the dividing surface. For classical systems, f_{ij} always takes a value between zero and one, and gives the temperature-dependent fraction of initial conditions on the dividing surface that initially point to products *and* eventually give rise to reaction.

When one has an educated guess regarding the reaction coordinate, but no knowledge of the transition state or the dividing surface, a reliable but computationally expensive solution is to calculate the free energy surface along a prescribed path from one free energy minimum to another. The free energy surface, $F(x_0)$, which is also known as the potential of mean force and as the reversible work surface, is given by:

$$F(x_0) = -k_B T \ln [L \langle \delta(x - x_0) \rangle] = -k_B T \ln Q(x_0), \quad (2.8)$$

where x is the assumed reaction coordinate, x_0 is the clamped value of x during the ensemble average over all other coordinates, the length L is a formal normalization constant that cancels when computing free energy differences, and $Q(x_0)$ is the partition function associated with the free energy at x_0 . In terms of the free energy surface, the TST rate constant is given by:

$$k_{i \rightarrow j}^{\text{TST}} = \frac{1}{2} \left(\frac{2k_B T}{\pi m} \right)^{1/2} \frac{e^{-\beta F(x^\ddagger)}}{\int_i dx e^{-\beta F(x)}}, \quad (2.9)$$

where the integral over x is restricted to the reactant region of configuration space. Computing TST rate constants is therefore equivalent to calculating free energy differences. Numerous methods have been developed over the years for computing $e^{-\beta F(x)}$, many of which fall under the name umbrella sampling or histogram window sampling.^{104,155,162}

While equations 2.6–2.9 are standard expressions of rare event theory, the exact way in which they are implemented depends strongly upon the actual system of interest. Indeed, if the transition state dividing surface is precisely known (as for the case of an adatom), then $k_{i \rightarrow j}^{\text{TST}}$ provides a good first approximation to the rate coefficient, and the dynamical correction factor accounts for the possibility that the particle does not thermalize in the state it has first reached, but instead goes on to a different final state. This process is called “dynamical recrossing” if the final state is identical to the original state, and otherwise is called “multisite jumping.” The importance of dynamical recrossing or multisite jumping depends on a number of factors, of which the height of the energy barriers and the mechanism of energy dissipation are essential.

For example, the minimum energy path for benzene to jump from a cation site to a window site in Na-Y is shown in figure 4, alongside the corresponding energy plot.³⁶ Despite benzene’s anisotropy, a reasonable model for the cation \leftrightarrow window dividing surface turns out to be the plane perpendicular to the three-dimensional vector connecting the two sites. This simple approach yields dynamical correction factors mostly above 0.5.³⁷

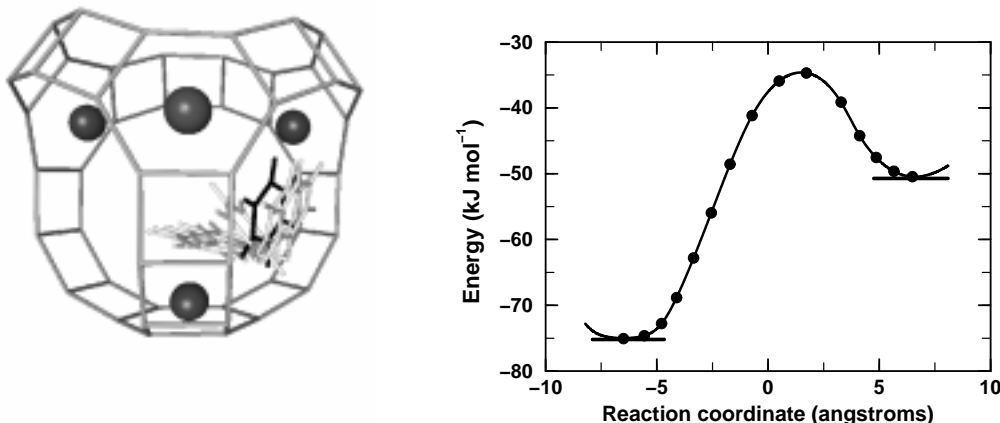


Figure 4. Cation \leftrightarrow window path for benzene in Na-Y (transition state indicated in bold), with a calculated barrier of 41 kJ mol^{-1} .³⁶

In a complex system with many degrees of freedom it might be difficult, or even impossible, to define rigorously the dividing surface between the states. In this case the transition state approximation may fail, requiring the calculation of f_{ij} . Indeed, TST assumes that all trajectories initially crossing the dividing surface in the direction of the product state will eventually relax in this state. This statement will be qualitatively false if the supposed surface does not coincide with the actual dividing surface. In this case, the dynamical correction factor corrects TST for an inaccurately defined dividing surface, even when dynamical recrossings through the actual dividing surface are rare. The problem of locating complex dividing surfaces has recently been addressed using topology,¹⁶³ statistics¹⁶⁴ and dynamics.^{165,166}

2. Recent Applications

Siliceous Zeolites. June, Bell and Theodorou reported the first application of TST dynamically corrected with RFMD for a zeolite-guest system in 1991,¹⁵³ modeling the diffusion of Xe and “spherical SF₆” in silicalite-1. This system is sufficiently weakly binding that reasonably converged MD simulations could be performed for comparison with the rare event dynamics, showing excellent quantitative agreement in the diffusivities obtained. The dynamical correction factors obtained by June *et al.* show that recrossings can diminish rate coefficients by as much as a factor of *ca.* 3, and that multisite jumps along straight channels in silicalite-1¹²⁴ contribute to the well known diffusion anisotropy in MFI-type zeolites.¹⁶⁷ Jousse and coworkers reported a series of MD studies on butene isomers in all-silica channel zeolites MEL and TON.^{123,168} Because the site-to-site energy barriers in these systems are comparable to the thermal energies studied in the MD simulations, rare event dynamics need not apply. Nonetheless, Jousse and coworkers showed that even for these relatively low-barrier systems, the magnitudes and loading dependencies of the MD diffusivities could be well explained within a jump diffusion model, with residence times extracted from the MD simulations.

As discussed in section II A 1, Snurr, Bell and Theodorou applied harmonic transition state theory (TST) to benzene diffusion in silicalite-1, assuming that benzene and silicalite-1 remain rigid, by using normal mode analysis for the 6 remaining benzene degrees of freedom.⁷² Their results underestimate experimental diffusivities by one to two orders of magnitude, probably more from assuming a rigid zeolite than from using harmonic TST. Forester and Smith subsequently applied TST to benzene in silicalite-1 using constrained reaction coordinate dynamics on both rigid and flexible lattices.⁷³ Lattice flexibility was found to have a very strong influence on the jump rates. Diffusivities obtained from the flexible framework simulations are in excellent agreement with experiment, overestimating the measured room temperature diffusivity ($2.2 \times 10^{-14} \text{ m}^2 \text{ s}^{-1}$) by only about 50%. These studies suggest that including framework flexibility is very important for bulkier guest molecules, which may require framework distortions to move along zeolite channels or through windows separating zeolite cages.

Cation-containing Zeolites. Mosell, Schrimpf and Brickmann reported a series of TST and RFMD calculations on Xe in Na-Y^{169,170} in 1996, and benzene and *p*-xylene in Na-Y^{59,60} in 1997. They calculated the reversible work of dragging a guest specie along the cage-to-cage [111] axis of Na-Y, and augmented this version of TST with dynamical corrections. In addition to computing the rate coefficient for cage-to-cage motion through Na-Y, Mosell *et al.* confirmed that benzene window sites are free energy local minima, while *p*-xylene window sites are free energy maxima, i.e. cage-to-cage transition states.^{59,60} Mosell *et al.* also found relatively small dynamical correction factors, ranging from 0.08–0.39 for benzene and 0.24–0.47 for *p*-xylene.

At about the same time in 1997, Jousse and Auerbach reported TST and RFMD calculations of specific site-to-site rate coefficients for benzene in Na-Y,³⁷ using equation 2.6 with jump-dependent dividing surfaces. As with Mosell *et al.*, we found that benzene jumps to window sites could be defined for all temperatures studied. We were unable to use TST to model the window \rightarrow window jump because we could not visualize simply the anisotropy of the window \rightarrow window dividing surface. For jumps other than window \rightarrow window, we found dynamical correction factors mostly above 0.5, suggesting that these jump-dependent dividing surfaces coincide closely with the actual ones. Although the flavors of the two approaches for modeling benzene in Na-Y differed, the final results were remarkably similar considering that different forcefields were used. In particular, Mosell *et al.* used MD to sample dividing surface configurations, while we applied the Voter displacement-vector Monte Carlo method¹⁶⁰ for sampling dividing surfaces. The apparent activation energy for cage-to-cage motion in our study is 44 kJ mol⁻¹, in very reasonable agreement with 49 kJ mol⁻¹ obtained by Mosell *et al.*

Finite Loadings. Tunca and Ford reported TST rate coefficients for Xe cage-to-cage jumps at high loadings in ZK-4 zeolite, the siliceous analog of Na-A (structure LTA).¹⁷¹ These calculations deserve several remarks. First, because this study treats multiple Xe atoms simultaneously, defining the reaction coordinate and dividing surface can become quite complex. Tunca and Ford addressed this problem by considering averaged cage sites, instead of specific intracage sorption sites, which is valid because their system involves relatively weak zeolite-guest interactions. They further assume a one-body reaction coordinate and dividing surface regardless of loading, which is tantamount to assuming that the window separating adjacent α -cages in ZK-4 can only hold one Xe at a time, and that cooperative

many-Xe cage-to-cage motions are unlikely. Second, Tunca and Ford advocate separate calculations of Q^\ddagger and Q_i for use in equation 2.7, as opposed to the conventional approach of calculating ratios of partition functions *viz.* free energies.¹⁶⁰ It is not yet obvious whether separating these calculations is worth the effort. Third, Tunca and Ford developed a recursive algorithm for building up $(N + 1)$ -body partition functions from N -body partition functions, using a “test particle” method developed for modeling the thermodynamics of liquids. Although the approach of Tunca and Ford has a restricted regime of applicability, it nonetheless seems promising in its direct treatment of many-body diffusion effects.

Free Energy Surfaces. Maginn, Bell and Theodorou performed reversible work calculations with a TST flavor on long chain alkanes in silicalite-1,¹³⁸ finding that diffusivities monotonically decrease with chain length until about n-C₈, after which diffusivities plateau and become nearly constant with chain length. Bigot and Peuch calculated free energy surfaces for the penetration of n-hexane and isooctane into a model of H-mordenite zeolite with an organometallic specie, Sn(CH₃)₃, grafted to the pore edge.¹⁷² Bigot and Peuch found that Sn(CH₃)₃ has little effect on the penetration barrier of n-hexane, but they predict that the organometallic increases the penetration barrier of isooctane by 60 kJ mol⁻¹. Sholl computed the free energy surface associated with particle exchange of Ar, Xe, methane and ethane in AlPO₄-5, a one-dimensional channel zeolite,¹⁷³ suggesting time scales over which anomalous single-file diffusion is expected in such systems.

Jousse, Auerbach and Vercauteren modeled benzene site-to-site jumps in H-Y zeolite (Si:Al=2.43), using a forcefield that explicitly distinguishes Si and Al, as well as oxygens in Si-O-Si, Si-O-Al and Si-OH-Al environments.³⁴ Such heterogeneity creates many distinct adsorption sites for benzene in H-Y. Multiple paths from site to site open as the temperature increases. To simplify the picture, we computed the free energy surface for benzene motion along the [111] axis in H-Y, which produces cage-to-cage migration. Due to the multiplicity of possible cage-to-cage paths, the temperature dependence of the cage-to-cage rate constant as computed by umbrella sampling exhibits strong non-Arrhenius behavior. These calculations may help to explain intriguing NMR correlations times for benzene in H-Y, which also exhibit striking non-Arrhenius temperature dependencies.⁴³

Quantum Dynamics. Of all the dynamics studies performed on zeolites, very few have explored the potentially quantum mechanical nature of nuclear motion in micropores.^{174–177} Quantum modeling of proton transfer in zeolites^{175,177,178} seems especially important because of its relevance in catalytic applications. Such modeling will become more prevalent in the near future, partially because of recent improvements in quantum dynamics approaches,¹⁷⁷ but mostly because of novel electronic structure methods developed by Sauer and coworkers,^{179,180} which can accurately compute transition state parameters for proton transfer in zeolites by embedding a quantum cluster in a corresponding classical forcefield.

To facilitate calculating quantum rates for proton transfer in zeolites, Fermann and Auerbach developed a novel semiclassical transition state theory (SC-TST) for truncated parabolic barriers,¹⁷⁷ based on the formulation of Hernandez and Miller.¹⁸¹ Our SC-TST rate coefficient is stable to arbitrarily low temperatures as opposed to purely harmonic SC-TST, and has the form $k^{\text{SC-TST}} = k^{\text{TST}} \cdot \Gamma$ where the quantum transmission coefficient, Γ , depends on the zero-point corrected barrier and the barrier curvature. To parameterize this calculation, Fermann, Blanco and Auerbach performed high level cluster calculations¹⁷⁸ yielding an O(1) \rightarrow O(4) zero-point corrected barrier height of 86.1 kJ mol⁻¹, which be-

comes 97.1 kJ mol^{-1} when including long range effects from the work of Sauer *et al.*¹⁷⁹ Using this new approach, Fermann and Auerbach calculated rate coefficients and crossover temperatures for the O(1) \rightarrow O(4) jump in H-Y and D-Y zeolites, yielding crossover temperatures of 368 K and 264 K, respectively. These results suggest that *tunneling dominates proton transfer* in H-Y up to and slightly above room temperature, and that true proton transfer barriers are being underestimated by neglecting tunneling in the interpretation of experimental mobility data.

III. LATTICE DYNAMICS IN ZEOLITES

When modeling strongly-binding or tight-fitting guest-zeolite systems, theoretical methods specialized for rare event dynamics such as TST and kinetic Monte Carlo (KMC) are required. These methods are applied by coarse-graining the molecular motions, keeping only their diffusive character. In zeolites, the well-defined cage and channel structure naturally orients this coarse-graining toward *lattice models*, which are the focus of this section.

The simplest such model was proposed by Ising in 1925.¹⁸² Many variants of the Ising model have since been applied to study activated surface diffusion.¹⁸³ Although in principle a lattice can be regarded simply as a numerical grid for computing configurational integrals required by statistical mechanics,¹⁸⁴ the grid points can have important physical meaning for dynamics in zeolites, as shown schematically in figure 5. Applying lattice models to diffusion in zeolites rests on several (often implicit) assumptions on the diffusion mechanism; here we recall those assumptions and analyze their validity for modeling dynamics of sorbed molecules in zeolites.

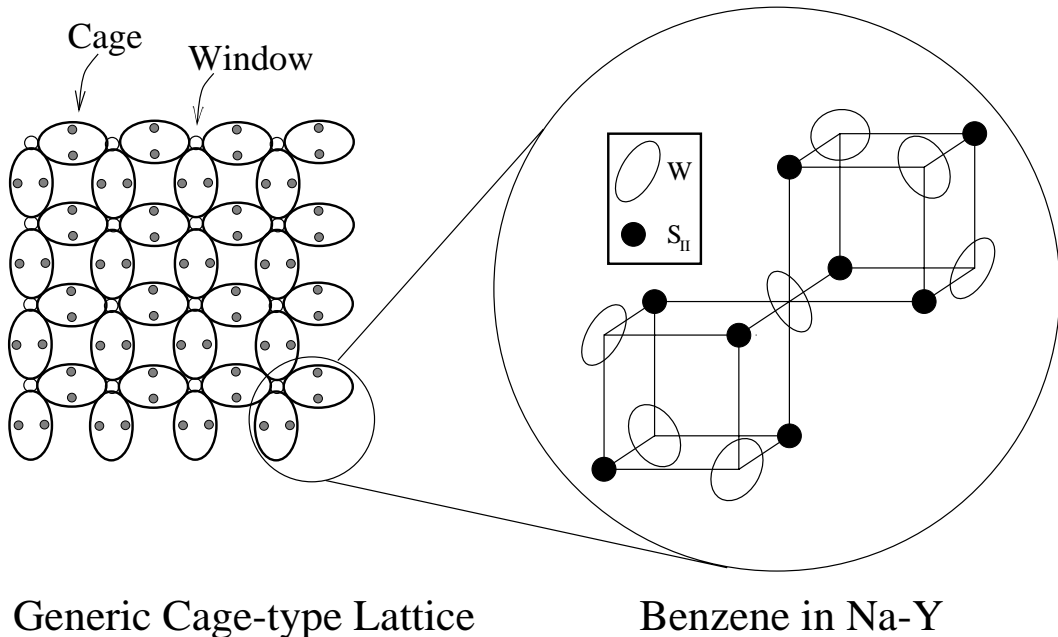


Figure 5. Schematic lattice model for molecules in cage-type zeolites, showing cages, intracage sites and window sites (left), as well as the specific lattice geometry for benzene in Na-Y zeolite (right).

A. Fundamental Assumptions

Temperature-independent Lattice. Lattice models of transport in zeolites begin by assuming that diffusion proceeds by activated jumps over free energy barriers between well-defined adsorption sites, i.e., that site residence times are much longer than travel times between sites. These adsorption sites are positions of high probability, constructed either from energy minima, for example next to cations in cation-containing zeolites, and/or from high volume, for example channel intersections in silicalite-1. Silicalite-1 provides a particularly illustrative example:⁷² its usual description in terms of adsorption sites involves two distinct channel sites, where the adsorbate is stabilized by favorable energy contacts with the walls of the 10R channels; and an intersection site at the crossing between the two channel systems, where the large accessible volume compensates entropically for less favorable contacts (see figure 6). Depending on the temperature, one or both types of sites can be populated simultaneously.

The silicalite-1 example points to the breakdown of the first assumption inherent in lattice models, namely, that adsorption and diffusion of guests in zeolites proceeds on a fixed lattice of sites, independent of external thermodynamic variables such as temperature. Clearly this is not the case. Indeed, when $k_B T$ becomes comparable with the activation energy for a jump from site i to site f , a new lattice that subsumes site i into site f may be more appropriate.¹²⁴ Alternatively, one may retain site i with modifications to the lattice model discussed below, taking into account so-called kinetic correlations that arise from the relatively short residence times in site i .^{123–125}

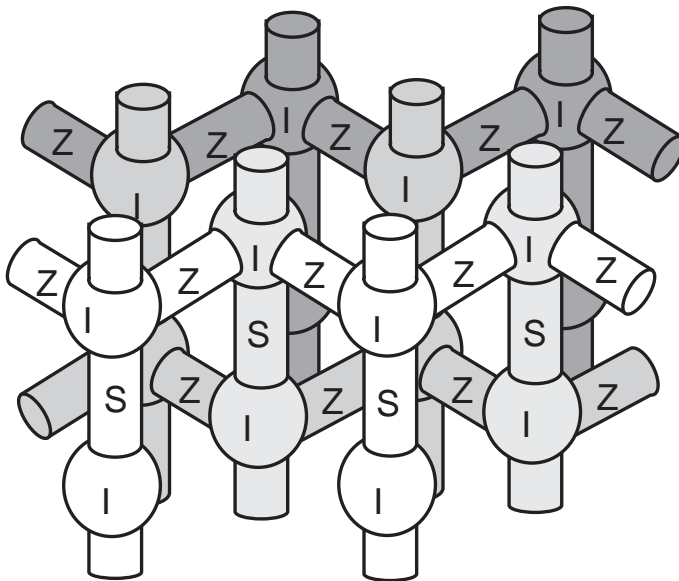


Figure 6. Channel and site structure of silicalite-1 showing intersection sites (I), straight channel sites (S) and zig-zag channel sites (Z).

Poisson Statistics. The second assumption inherent in most lattice models of diffusion, which is related to the first, is that subsequent jumps of a given molecule are uncorrelated from each other, i.e., that a particular site-to-site jump has the same probability to occur at any time. This assumption results in a site residence time distribution that follows the

exponential law associated with Poisson statistics.¹⁸⁵ In figure 2 we have seen that such a law can indeed result from the analysis of MD trajectories. As a result, lattice models can often be mapped onto master rate equations such as those in the chemical kinetics of first-order reactions.^{185,186} This fact highlights the close connection between reaction and diffusion in zeolites, when modeled with lattice dynamics.

This second assumption obtains from the following physical observations. Time-independent jump probabilities arise when the mechanism of activation involves simple energy transfer from the heat bath, which is usually *very* rapid compared to site-to-site jumping. Subsequent jumps are uncorrelated when center-of-mass velocity correlations of the jumping guest decay well before the next jump occurs. Both of these criteria are typically satisfied when free energy minima are very deep compared to $k_B T$. However, when $k_B T$ becomes comparable to barriers separating sites, multisite jumps become important,^{187–191} requiring either the definition of a more coarse-grained lattice,¹²⁴ the calculation of multisite jump rates,¹⁹² or a statistical model that estimates the kinetic correlations between subsequent jumps.^{123,125,193} We have found that ignoring multisite jumps yields accurate results for diffusion through cage-type zeolites such as Na-Y,³⁷ but that such an approximation can cause noticeable errors for transport through channel zeolites such as silicalite-1 (MFI) and silicalite-2 (MEL).^{123,125}

Deviations from Poisson statistics would also arise if a molecule were most likely to jump in phase with a low frequency zeolite framework vibration, such as a window breathing mode,¹⁹⁴ or if a molecule were most likely to jump in concert with another guest molecule. An extreme case of this latter effect was predicted by Sholl and Fichthorn,^{65,152} wherein strong adsorbate-adsorbate interactions in single-file zeolites generated transport dominated by correlated cluster dynamics instead of single molecule jumps. In this case, a consequence of Poisson statistics applied to diffusion in zeolites at finite loadings ceases to hold, namely, there no longer exists a time interval sufficiently short so that only one molecule can jump at a time.

Loading-independent Lattice. The final assumption, which is typically invoked by lattice models of diffusion at finite loadings, is that the sites do not qualitatively change their nature with increasing adsorbate loading. This assumption holds when adsorption sites are separated by barriers such as windows between large cages,¹⁷¹ and also when host-guest interactions dominate guest-guest interactions. This loading-independent lattice model breaks down when the effective diameter of guest molecules significantly exceeds the distance between adjacent adsorption sites, as high loadings create unfavorable excluded-volume interactions between adjacent guests. This effect does not arise for benzene in Na-Y,¹⁹⁵ which involves site-to-site distances and guest diameters both around 5 Å, but is predicted for Xe in Na-A by classical density functional theory calculations.¹⁹⁶

Despite these many caveats, lattice models have proven extremely useful for elucidating qualitatively and even semi-quantitatively the following physical effects regarding: (*i*) host structure: pore topology,^{197–199} diffusion anisotropy,^{167,200} pore blockage,²⁰¹ percolation,²⁰² and open system effects;^{16,200} (*ii*) host-guest structure: site heterogeneity^{203,204} and reactive systems;²⁰⁵ and (*iii*) guest-guest structure: attractive interactions,^{168,198,199} phase transitions,^{206,207} concerted cluster dynamics,^{65,152} single-file diffusion,^{16,208} and diffusion of mixtures.^{144,209,210} In what follows, we outline the theory and simulation methods used to address these issues.

B. Kinetic Monte Carlo

In section II C we outlined dynamical methods for computing site-to-site jump rate coefficients for molecules in zeolites. In order to make contact with measurements of transport through zeolites,^{8,9} we must relate these site-to-site rate coefficients with quantities such as the self diffusivity and transport diffusivity, which arise from molecular translation; or we can model NMR correlation times, which are controlled by molecular rotation. At infinite dilution on an M -dimensional hypercubic lattice, i.e. 1-d, 2-d square, 3-d cubic, etc., both the self and transport diffusivity are given by $D_0 = k_{\text{hop}}a^2 = \frac{1}{2M}ka^2$, where k_{hop} is the fundamental rate coefficient for jumps between nearest neighbor sites, a is the distance between such sites, and $1/k$ is the mean site residence time.¹⁸³ This result neglects multisite hops, which have jump distances greater than a . An alternative formula exists that accounts for such jumps in terms of multisite jump rates.

Unfortunately, site lattices in zeolites are usually much more complicated than hypercubic, apparently defying such simple analytical formulas. To address this complexity, many researchers have applied kinetic Monte Carlo (KMC) to model diffusion in zeolites, parameterized either by *ad hoc* jump frequencies or by atomistically calculated jump rate coefficients. KMC models diffusion on a lattice as a random walk composed of uncorrelated, single molecule jumps as discussed above, thereby providing a stochastic solution to the master equation associated with the lattice model. Although KMC models transport as sequences of uncorrelated events in the sense that jump times are extracted from Poisson distributions, KMC does account for spatial correlations at finite loadings. Indeed, when a molecule executes a jump at higher loadings, it leaves behind a vacancy that is likely to be occupied by a successive jump, thereby diminishing the diffusivity from the mean field theory estimate discussed in section III C.

KMC is isomorphic to the more conventional Monte Carlo algorithms,⁸⁵ except that in a KMC simulation random numbers are compared to ratios of rate coefficients, instead of ratios of Boltzmann factors. However, if the pre-exponential factors cancel in a ratio of rate coefficients, then a ratio of Boltzmann factors does arise, where the relevant energies are *activation energies*. KMC formally obeys detailed balance, meaning that all thermodynamic properties associated with the underlying lattice Hamiltonian can be simulated with KMC. In addition to modeling transport in zeolites, KMC has been used to model adsorption kinetics on surfaces,²¹¹ and even surface growth itself.²¹²

1. Algorithms and Ensembles

Algorithms. KMC can be implemented with either constant time-step or variable time-step algorithms. Variable time-step methods are efficient for sampling jumps with widely varying time scales, while fixed time-step methods are convenient for calculating ensemble averaged correlation functions. In the constant time-step technique, jumps are accepted or rejected based on the kinetic Metropolis prescription, in which a ratio of rate coefficients, $k_{\text{hop}}/k_{\text{ref}}$, is compared to a random number.^{39,213} Here k_{ref} is a reference rate that controls the temporal resolution of the calculation according to $\Delta t_{\text{bin}} = 1/k_{\text{ref}}$. The probability to make a particular hop is proportional to $k_{\text{hop}}/k_{\text{ref}}$, which is independent of time, leading

naturally to a Poisson distribution of jump times in the simulation. In the fixed time-step algorithm, all molecules in the simulation attempt a jump during the time Δt_{bin} . In order to accurately resolve the fastest molecular jumps, k_{ref} should be greater than or equal to the largest rate constant in the system, in analogy with choosing time steps for MD simulations. However, if there exists a large separation in time scales between the most rapid jumps, e.g. intracage motion, and the dynamics of interest, e.g. cage-to-cage migration, then one may vary k_{ref} to improve efficiency. The cost of this modification is detailed balance; indeed, tuning k_{ref} to the dynamics of interest is tantamount to simulating a system where all the rates larger than k_{ref} are replaced with k_{ref} .

A useful alternative for probing long-time dynamics in systems with widely varying jump times is variable time-step KMC. In the variable time-step technique, a hop is made every KMC step and the system clock is updated accordingly.^{201,214} For a given configuration of random walkers, a process list of possible hops from occupied to empty sites is compiled for all molecules. A particular jump from site i to j is chosen from this list with a probability of $k_{i \rightarrow j}/k_{\text{tot}}$, where k_{tot} is the sum of all rate coefficients in the process list. In contrast to fixed time-step KMC, where *all* molecules *attempt* jumps during a KMC step, in variable time-step KMC a *single* molecule *executes* a jump every KMC step and the system clock is updated by an amount $\Delta t_n = -\ln(1-x)/k_{\text{tot}}$, where $x \in [0,1)$ is a uniform random number and n labels the KMC step. This formula results directly from the Poisson distribution, suggesting that other formulas may be used in variable time-step KMC to model kinetic correlations.¹²³ In general, we suggest that simulations be performed using the variable time-step method, with data analyses carried out by mapping the variable time-step KMC trajectories onto a fixed time-step grid¹⁸⁶ as discussed in section III B 2.

Ensembles. Guest-zeolite systems at equilibrium are inherently multicomponent systems at constant temperature and pressure. Since guest molecules are continually adsorbing and desorbing from more-or-less fixed zeolite particles, a suitable ensemble would fix $N_Z =$ amount of zeolite, $\mu_G =$ chemical potential of guest, $p =$ pressure and $T =$ temperature, keeping in mind that μ_G and p are related by the equation of state of the external fluid phase. However, constant-pressure simulations are very challenging for lattice models, since constant pressure implies volume fluctuations, which for lattices involve adding or deleting whole adsorption sites. As such, constant-volume simulations are much more natural for lattice dynamics. Since both the volume and amount of zeolite is virtually fixed during intracrystalline adsorption and diffusion of guests, we need to specify only one of these variables. In lattice simulations it is customary to specify the number of adsorption sites, N_{sites} , which plays the role of a unitless volume. We thus arrive at the natural ensemble for lattice dynamics in zeolites: the grand canonical ensemble, which fixes μ_G , N_{sites} and T .

The overwhelming majority of KMC simulations applied to molecules in zeolites have been performed using the canonical ensemble, which fixes $N_G =$ number of guest molecules, N_{sites} and T . Although the adsorption-desorption equilibrium discussed above would seem to preclude using the canonical ensemble, fixing N_G is reasonable if zeolite particles are large enough to make the relative root mean square fluctuations in N_G rather small. Such closed-system simulations are usually performed with periodic boundary conditions, in analogy with atomistic simulations.^{85,104} Defining the fractional loading, θ , by $\theta \equiv N_G/N_{\text{sites}}$, typical KMC calculations produce the self-diffusion constant D_s as a function of T at fixed θ for Arrhenius analysis, or as a function of θ at fixed T , a so-called diffusion isotherm.

There has recently been renewed interest in grand canonical KMC simulations for three principal reasons: to relax periodic boundary constraints to explore single-file diffusion with lattice dynamics,¹⁶ to study non-equilibrium permeation through zeolites membranes,²⁰⁰ and in general to explore the interplay between adsorption and diffusion in zeolites.^{140,215,216} Grand canonical KMC requires that the lattice contain at least one edge that can exchange particles with an external phase. In contrast to grand canonical MC used to model adsorption, where particle insertions and deletions can occur anywhere in the system, grand canonical KMC must involve insertions and deletions only at the edges in contact with external phases, as shown in figure 8.

The additional kinetic ingredients required by grand canonical KMC are the rates of adsorption to and desorption from the zeolite.²¹⁷ Because desorption generally proceeds with activation energies close to the heat of adsorption, desorption rates are reasonably simple to estimate. However, adsorption rates are less well-known, because they depend on details of zeolite crystallite surface structure. Although qualitative insights on rates of penetration into microporous solids are beginning to emerge,^{218,219} zeolite-specific models have yet to take hold.¹⁷² Calculating precise adsorption rates may not be crucial for parameterizing qualitatively reliable simulations, because adsorption rates are typically much larger than other rates in the problem. For sufficiently simple lattice models, adsorption and desorption rates can be balanced to produce the desired loading according to the adsorption isotherm.²⁰⁰ If one assumes that the external phase is an ideal fluid, then insertion frequencies are proportional to pressure p . As such, equilibrium grand canonical KMC produces the self-diffusion coefficient as a function of p and T . Alternatively, for non-equilibrium systems involving different insertion frequencies on either site of the membrane, arising from a pressure (chemical potential) gradient across the membrane, grand canonical KMC produces the Fickian or transport diffusion coefficient, D , as a function of T and the local loading in the membrane.

2. Data Analyses

Computing ensemble averages and correlation functions is extremely straightforward using fixed time-step KMC. Ensemble averages take the form:

$$\langle A \rangle = \frac{1}{T_K} \sum_{n=1}^{N_F} \Delta t_{\text{bin}} A(n) = \frac{1}{N_F} \sum_{n=1}^{N_F} A(n), \quad (3.1)$$

where $T_K = N_F \Delta t_{\text{bin}}$ is the total KMC time elapsed in a fixed time-step simulation, N_F is the number of steps in the fixed time-step simulation, and $A(n)$ is some dynamical variable evolving during the KMC trajectory. In addition, correlation functions are obtained according to:

$$C(t) = \langle A(0)B(t) \rangle = \frac{1}{N_F} \sum_{n=1}^{N_F-m} A(n)B(n+m), \quad (3.2)$$

where $t = m \Delta t_{\text{bin}}$. Ensemble averages from variable time-step KMC take the form:

$$\langle A \rangle = \frac{1}{T_K} \sum_{n=1}^{N_V} \Delta t_n A(n), \quad (3.3)$$

where N_V is the number of steps in a variable time-step simulation, and Δt_n are the variable time steps. We note that while the physical time T_K may not vary between fixed and variable time-step simulations, the numbers of steps, N_F and N_V respectively, will generally be different because each fixed time-step involves a full system sweep, while each variable time-step effects a single molecule jump.

Computing correlation functions with variable time steps is not as straightforward as that for ensemble averages. We first choose a time bin width, Δt_{bin} , which must be adjusted to encompass the dynamics we wish to study. For example, Δt_{bin} should be a fraction of the estimated cage residence time when modeling diffusion in cage-type zeolites.²⁰³ For the time $t = n\Delta t_{\text{bin}}$, the correlation function $C(t)$ is given by:

$$C(t) = \langle A(0)B(t) \rangle = \frac{1}{Q_n} \sum'_{lm} A(l)B(m), \quad (3.4)$$

where the sum is restricted to those pairs (l, m) for which $t_m - t_l$ falls into the n^{th} time bin, characterized by $n = \text{int}[(t_m - t_l)/\Delta t_{\text{bin}}]$, and Q_n is the number of such pairs.

Probably the most important quantity that is calculated from a KMC simulation is the MSD, which was discussed in section II B 2. The long-time limit required to relate the MSD to diffusion vindicates the use of time bins that contaminate short-time dynamics, as can arise for both fixed and variable time-step KMC. The MSD is calculated with variable time-step KMC by replacing $A(l)B(m)$ in equation 3.4 with $|\mathbf{r}(l) - \mathbf{r}(m)|^2$. Great care must be taken to ensure that KMC simulations are run long enough to approach the long-time limit implicit in the Einstein relation. Indeed, one can obtain linear MSDs and still *not* sample truly diffusive motion through zeolites.³⁹

To make direct contact with NMR probes of dynamics²²⁰ such as NMR relaxation,^{43,221} exchange-induced sidebands NMR,¹⁰ and multidimensional exchange NMR,²²² one can use KMC to calculate the orientational correlation function (OCF) given by $C(t) = \langle P_2(\cos \beta_t) \rangle$, where $P_2(x) = \frac{1}{2}(3x^2 - 1)$ is the second-degree Legendre polynomial, and β_t is the angle between a molecular axis at time 0 and t . In practice, an efficient way to evaluate OCFs using KMC is to pre-compute and store a matrix of values of $P_2[\cos \beta(ij)]$, where i and j label different sites in the lattice. In analogy with equation 3.4, the KMC-calculated OCF thus becomes:

$$C(t) = \frac{1}{Q_n} \sum'_{lm} P_2[\cos \beta(i_l j_m)], \quad (3.5)$$

where i_l is the site occupied at time t_l , and likewise for j_m . Calculating OCFs at long times with KMC is typically more computationally intensive than that for MSDs, because Monte Carlo algorithms are generally inefficient at converging exponentially small numbers arising from sign cancellation. This is known as the “sign problem” which is especially dire for real-time quantum Monte Carlo and many-fermion quantum Monte Carlo. In actual applications, Auerbach and coworkers have used brute-force computer power to converge OCFs,^{39,186} which severely limits the system sizes one can study.

3. Models of Finite Loading

The great challenge in performing KMC simulations at finite loadings is that the rate coefficients $\{k_{i \rightarrow j}\}$ should depend upon the local configuration of molecules because of guest-guest interactions. That is, in compiling the process list of allowed jumps and associated rate constants on the fly of a KMC simulation, TST or related calculations should be performed to account for the effect of specific guest configurations on the jump rate coefficients. To date, this “*ab initio* many-body KMC” approach has not been employed because of its daunting computational expense. Instead, researchers either ignore how guest-guest interactions modify rate coefficients for site-to-site jumps; or they use many-body MD at elevated temperatures when guest-guest interactions cannot be ignored.^{165,166}

A popular approach for modeling many-body diffusion in zeolites with KMC is thus the “site blocking model,” where guest-guest interactions are ignored, except for exclusion of multiple site occupancy. This model accounts for entropic effects of finite loadings, but not energetic effects. Calculating the process list and available rate coefficients becomes particularly simple; one simply sums the available processes using rates calculated at infinite dilution.²²³ This model is attractive to researchers in zeolite science,²²⁴ because blocking of cage windows and channels by large, aromatic molecules that form in zeolites, i.e. “coking,” is a problem that zeolite scientists need to understand and eventually control.

The site blocking model ignores guest-guest interactions that operate over medium to long length scales, which modify jump activation energies for site-to-site rate coefficients depending upon specific configurations of neighboring adsorbates. By incorporating these additional interactions, diffusion models reveal the competition between guest-zeolite adhesion and guest-guest cohesion.^{168,225,226} Qualitatively speaking, the diffusivity is generally expected to increase initially with increasing loading when repulsive guest-guest interactions decrease barriers between sites, and to decrease otherwise. At very high loadings, site blocking lowers the self diffusivity regardless of the guest-guest interactions.

To develop a quantitative model for the effects of guest-guest attractions Saravanan *et al.* proposed a “parabolic jump model,” which relates binding energy shifts to transition state energy shifts.^{203,227} This method was implemented for lattice gas systems whose thermodynamics is governed by the following Hamiltonian:

$$H(\vec{n}) = \sum_{i=1}^M n_i f_i + \frac{1}{2} \sum_{i,j=1}^M n_i J_{ij} n_j, \quad (3.6)$$

where M is the number of sites in the lattice, $\vec{n} = (n_1, n_2, \dots, n_M)$ are site occupation numbers listing a configuration of the system, and $f_i = \varepsilon_i - Ts_i$ is the free energy for binding in site i . In equation 3.6, J_{ij} is the nearest neighbor interaction between sites i and j , i.e. $J_{ij} = 0$ if sites i and j are not nearest neighbors.

Saravanan *et al.* assumed that the minimum energy hopping path connecting adjacent sorption sites is characterized by intersecting parabolas, shown in figure 7, with the site-to-site transition state located at the intersection point. For a jump from site i to site j , with $i, j = 1, \dots, M$, the hopping activation energy including guest-guest interactions is given by:

$$E_a(i, j) = E_a^{(0)}(i, j) + \Delta E_{ij} \left(\frac{1}{2} + \frac{\delta E_{ij}^{(0)}}{k_{ij} a_{ij}^2} \right) + \Delta E_{ij}^2 \left(\frac{1}{2k_{ij} a_{ij}^2} \right), \quad (3.7)$$

where $E_a^{(0)}(i, j)$ is the infinite dilution activation energy calculated using the methods of section II C, and a_{ij} is the jump distance. ΔE_{ij} is the *shift* in the energy difference between sites i and j resulting from guest-guest interactions, and is given by $\Delta E_{ij} = (E_j - E_i) - (\varepsilon_j - \varepsilon_i)$, where $E_k = \varepsilon_k + \sum_{l=1}^M J_{kl}n_l$. This method allows the rapid estimation of configuration dependent barriers during a KMC simulation, knowing only infinite dilution barriers and the nearest neighbor interactions defined above. The parabolic jump model is most accurate when the spatial paths of jumping molecules are not drastically changed by guest-guest interactions, although the energies can change as shown in figure 7. While other lattice models of diffusion in zeolites have been proposed that account for guest-guest attractions,^{168,226} the parabolic jump model has the virtue of being amenable to analytical solution, as discussed in section III C 1.

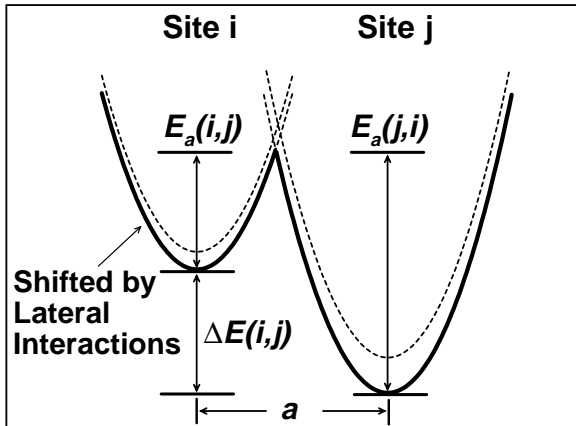


Figure 7. Site-to-site jump activation energies perturbed by guest-guest interactions, approximated with parabolic jump model.

4. Recent Applications

Infinite Dilution. Most KMC simulations of diffusion in zeolites are performed at high guest loadings, to explore the effects on transport of guest-guest interactions. A handful of KMC studies have been reported at infinite dilution, to relate fundamental rate coefficients with observable self diffusivities for particular lattice topologies. June *et al.* augmented their TST and RFMD study with KMC calculations of Xe and SF₆ self diffusivities in silicalite-1.¹⁵³ They obtained excellent agreement among apparent activation energies for Xe diffusion calculated using MD, KMC with TST jump rates, and KMC with RFCT jump rates. The resulting activation energies fall in the range 5–6 kJ mol⁻¹, which is much lower than the experimentally determined values of 15 and 26 kJ mol⁻¹.^{228,229} van Tassel *et al.* reported a similar study in 1994 on methane diffusion in zeolite A, finding excellent agreement between self diffusivities calculated with KMC and MD.²³⁰

Auerbach *et al.* reported KMC simulations of benzene diffusion in Na-Y showing that the cation → window jump (see figure 4) controls the temperature dependence of diffusion, with a predicted activation energy of 41 kJ mol⁻¹.³⁶ Because benzene residence times at cation sites are so long, these KMC studies could not be compared directly with MD, but nonetheless

yield reasonable agreement with the QENS barrier of 34 kJ mol⁻¹ measured by Jobic *et al.*⁴⁵ Auerbach and Metiu then reported KMC simulations of benzene orientational randomization in various models of Na-Y with different numbers of supercage cations, corresponding to different Si:Al ratios.³⁹ Full cation occupancy gives randomization rates controlled by intracage motion, whereas half cation occupancy gives rates sensitive to *both* intracage and intercage motion. This finding prompted Chmelka and coworkers to perform exchange-induced sidebands NMR experiments on labeled benzene in the corresponding Ca-Y (Si:Al=2.0), finding indeed that they were able to measure both the cation → cation and cation → window jump rates within a single experiment.¹⁰ Finally, when Auerbach and Metiu modeled benzene orientational randomization with one quarter cation occupancy, they found *qualitative sensitivity* to different spatial patterns of cations, suggesting that measuring orientational randomization in zeolites can provide important information regarding cation disorder and possibly Al distributions.

Finite Loadings. Theodorou and Wei used KMC to explore a site blocking model of reaction and diffusion with various amounts of coking.²⁰⁹ Nelson and coworkers developed similar models, to explore the relationship between the catalytic activity of a zeolite and its lattice percolation threshold.^{231,232} In a related study, Keffer, McCormick and Davis modeled binary mixture transport in zeolites, where one component diffuses rapidly while the other component is trapped at sites, e.g. methane and benzene in Na-Y.²⁰² They used KMC to calculate percolation thresholds of the rapid penetrant as a function of blocker loading, and found that these thresholds agree well with predictions from simpler percolation theories.²³³

Coppens, Bell and Chakraborty used KMC to calculate the loading dependence of self diffusion for a variety of lattices, for comparison with mean field theories (MFT) of diffusion (see section III C 1).¹⁹⁷ These theories usually predict $D_s(\theta) \cong D_0(1 - \theta)$, where θ is the fractional occupancy of the lattice and D_0 is the self diffusivity at infinite dilution. Coppens *et al.* found that the error incurred by MFT is greatest for lattices with low coordination numbers, such as silicalite-1 and other MFI-type zeolites. Coppens *et al.* then reported KMC simulations showing that by varying the concentrations of weak and strong binding sites,²⁰⁴ their system exhibits most of the loading dependencies of self diffusion reported by Kärger and Pfeifer.²³⁴ Bhide and Yashonath also used KMC to explore the origins of the observed loading dependencies of self diffusion, finding that most of these dependencies can be generated by varying the nature and strength of guest-guest interactions.^{198,199}

Benzene in Na-X. Auerbach and coworkers reported a series of studies modeling the concentration dependence of benzene diffusion in Na-X and Na-Y zeolites.^{195,203,223,227,235} These studies were motivated by persistent, qualitative discrepancies between different experimental probes of the coverage dependence of benzene self diffusion in Na-X.⁸ Pulsed field gradient (PFG) NMR diffusivities decrease monotonically with loading for benzene in Na-X,²³⁶ while tracer zero-length column (TZLC) data *increase* monotonically with loading for the same system.²³⁷ We performed KMC simulations using the parabolic jump model to account for guest-guest attractions.^{203,227} Our KMC results for benzene in Na-X are in excellent qualitative agreement with the PFG NMR results, and in qualitative disagreement with TZLC. Other experimental methods yield results for benzene in Na-X that also agree broadly with these PFG NMR diffusivities.^{41,238,239} Although the evidence appears to be mounting in favor of the PFG NMR loading dependence for benzene in Na-X, it remains unclear just what is being observed by the TZLC measurements. To address this issue, Brandani *et al.*

reported TZLC measurements for benzene in various Na-X samples with different particle sizes. They found tracer exchange rates that exhibit a normal dependence on particle size, suggesting that their diffusivities are free from artifacts associated with unforeseen diffusion resistances at zeolite crystallite surfaces.²³⁷

Noting that molecular transport in TZLC measurements samples longer length scales than that in PFG NMR experiments, Chen *et al.* have suggested that the TZLC method may be more sensitive than is PFG NMR to electrostatic traps created by random Al and cation distributions.⁴⁸ By performing a field theory analysis of an augmented diffusion equation, Chen *et al.* estimate that such charge disorder can diminish the self diffusivity by roughly two orders of magnitude from that for the corresponding ordered system. This effect is remarkably close to the discrepancy in absolute magnitudes between PFG NMR and TZLC diffusivities for benzene in Na-X at low loadings.²³⁷ This intriguing prediction by Chen *et al.* suggests that there should be a striking difference between benzene diffusion in Na-X (Si:Al=1.2) and in Na-LSX (Si:Al=1), since the latter is essentially an ordered structure. We are not aware of self diffusion measurements for benzene in Na-LSX, but we can turn to NMR spin-lattice relaxation data for deuterated benzene in these two zeolites.^{18,240} Unfortunately, such data typically reveal only short length scale, intracage dynamics,³⁹ and as a result may not provide such a striking effect. Indeed, the activation energy associated with the NMR correlation time changes only moderately, decreasing from 14.0 ± 0.6 kJ mol⁻¹ for Na-X¹⁸ to 10.6 ± 0.9 kJ mol⁻¹ for Na-LSX,²⁴⁰ in qualitative agreement with the ideas of Chen *et al.*⁴⁸ It remains to be seen whether such electrostatic traps can explain the loading dependence observed by TZLC for benzene in Na-X.

By varying fundamental energy scales, the model of Saravanan and Auerbach for benzene in FAU-type zeolites exhibits four of the five loading dependencies of self diffusion reported by Kärger and Pfeifer,²³⁴ in analogy with the studies of Coppens *et al.*²⁰⁴ and Bhide and Yashonath.^{198,199} However, in contrast to these other KMC studies, we have explored the role of phase transitions^{206,207} in determining the loading dependencies of self diffusion.²⁰³ In particular, we find that Kärger and Pfeifer’s type III diffusion isotherm, which involves a nearly constant self diffusivity at high loadings, may be characteristic of a cluster-forming, subcritical adsorbed phase where the cluster of guest molecules can extend over macroscopic length scales. Such cluster formation suggests a diffusion mechanism involving “evaporation” of particles from clusters. Although increasing the loading in subcritical systems increases cluster sizes, we surmise that evaporation dynamics remains essentially unchanged by increasing loading. As such, we expect the subcritical diffusivity to obtain its high loading value at low loadings, and to remain roughly constant up to full loading. In addition, we find that Kärger and Pfeifer’s types I, II and IV are characteristic of supercritical diffusion, and can be distinguished based on the loading that gives the maximum diffusivity, θ_{\max} . For example, the PFG NMR results discussed above for benzene in Na-X are consistent with $\theta_{\max} \lesssim 0.3$, while the TZLC data give $\theta_{\max} \gtrsim 0.5$. Our simulations predict that θ_{\max} will decrease with increasing temperature, increasing strength of guest-guest attractions, decreasing free energy difference between site types, and in general anything that makes sites more equally populated.²⁰³

Reactive Systems. Trout, Chakraborty and Bell applied electronic structure methods to calculate thermodynamic parameters for possible elementary reactions in the decomposition of NO_x over Cu-ZSM-5.²⁴¹ Based on these insights, they developed a KMC model of reac-

tion and diffusion in this system, seeking the optimal distribution of isolated reactive Cu centers.²⁰⁵ This hierarchical approach to realistic modeling of complex systems presents an attractive avenue for future research.

Open Systems. Gladden *et al.* developed a versatile open-system KMC program that allows them to study adsorption, diffusion and reaction in zeolites simultaneously.²¹⁶ They have applied their algorithm to model ethane and ethene binary adsorption in silicalite-1,²¹⁶ finding excellent agreement with the experimental binary isotherm.

Nelson and Auerbach reported open-system KMC simulations of anisotropic diffusion²⁰⁰ and single-file diffusion¹⁶ (infinitely anisotropic) through zeolite membranes. They defined an anisotropy parameter, η , according to $\eta = k_y/k_x$, where k_x and k_y are the elementary jump rates in the transmembrane and in-plane directions, respectively, as shown in figure 8. For example, the $\eta < 1$ case models *p*-xylene permeation through a silicalite-1 membrane (see figure 6) oriented along the the straight channels (*b*-axis), while $\eta > 1$ corresponds to the same system except oriented along the the zig-zag (*a*-axis) or “corkscrew” channels (*c*-axis).¹⁰⁹ The limiting case $\eta = 0$ corresponds to single-file diffusion.

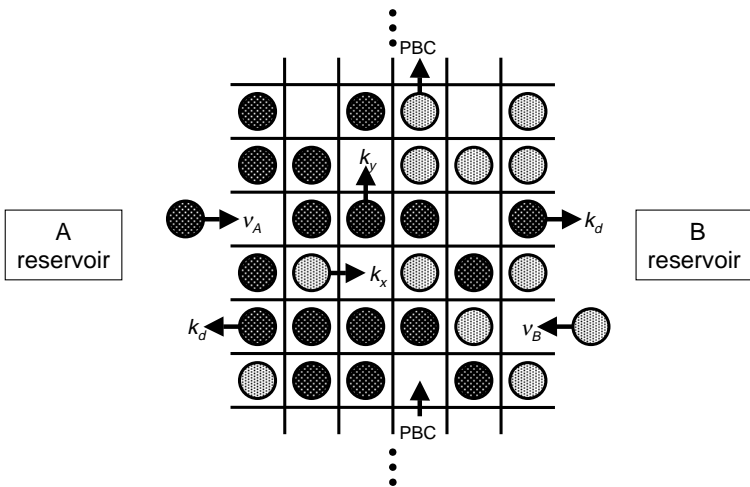


Figure 8. Schematic of a tracer counter-permeation simulation, with identical but differently labeled particles. Diffusion anisotropy is controlled by the parameter $\eta = k_y/k_x$, with the limiting case $\eta = 0$ corresponding to single-file diffusion.

Nelson and Auerbach have studied how the self diffusivity depends upon membrane thickness L , and anisotropy η . However, the long-time limit of the MSD may not be accessible in a membrane of finite thickness. Furthermore, the natural observable in a permeation measurement is steady-state flux rather than the MSD. To address these issues, they simulated two-component, equimolar counter-permeation of identical, labeled species—i.e. tracer counter-permeation—which has been shown to yield transport identical to self diffusion.²⁴² Such a situation is closely related to the tracer zero-length column experiment developed

by Ruthven and coworkers.²³⁷ When normal diffusion holds the self diffusivity is independent of membrane thickness, while anomalous diffusion is characterized by an L -dependent self diffusivity. For $\eta \gg 1$, Nelson and Auerbach found that diffusion is normal and that MFT becomes exact in this limit,²⁰⁰ i.e. $D_s(\theta) = D_0(1 - \theta)$. This is because sorbate motion in the plane of the membrane is very rapid, thereby washing out any correlations in the transmembrane direction. As η is reduced, correlations between the motion of nearby molecules decrease the diffusivity. For small values of η , a relatively large lattice is required to reach the thick membrane limit, such that particle exchange becomes probable during the intracrystalline lifetime. The extreme case of this occurs when $\eta = 0$, for which diffusion is strictly anomalous for all membrane thicknesses.

Nelson *et al.* applied their open-system KMC algorithm to study the nature of anomalous diffusion through single-file zeolites of finite extent.¹⁶ For times shorter than the vacancy diffusion time, $t_c = L^2/\pi D_0$, particle transport proceeds via the non-Fickian, single-file diffusion mode, with mean square displacements increasing with the square-root of time. For times longer than t_c , however, we find that self diffusion in single-file systems is completely described by Fick’s laws, except that the “Fickian” self diffusion constant depends on file length, scaling inversely with L for long files. This gives an intracrystalline residence time, $\tau_{\text{intra}} \equiv L^2/D_s$, that scales with L^3 for long files, in complete agreement with the mean field analysis reported by Rodenbeck and Kärger.²⁴³ Nelson and Auerbach found that the fraction of time in the single-file diffusion mode scales inversely with file length for long files, suggesting that Fickian self diffusion *dominates transport* in longer single-file zeolites. They predicted that the cross-over time between (medium time) single-file diffusion and (long time) Fickian diffusion is just above the experimental window for PFG NMR experiments, suggesting that longer-time PFG NMR would observe this transition.

C. Mean Field and Continuum Theories

Mean field theory (MFT) and continuum theories provide illustrative and efficient means for estimating the results of KMC simulations. MFT reduces the complexity of many-body structure and dynamics to the simplicity of effective one-body properties,¹⁵⁵ by averaging over local fluctuations in the instantaneous energy of each adsorption site. Although MFT can give numerical error for lattices with low coordination,¹⁹⁷ the theory remains qualitatively reliable except near critical points, where cooperative fluctuations extend over large distances. MFT can thus serve as a useful launching point for an analytical theory of many-body diffusion in zeolites.

1. Finite Loading Effects

For diffusion at finite loadings on a hypercubic lattice within the site blocking model, MFT predicts that $D_s(\theta) \cong D_0(1 - \theta)$, where θ is the fractional occupancy of the lattice and D_0 is the self diffusivity at infinite dilution. The factor $(1 - \theta)$ is the fraction of jumps that are successful at finite loadings, because they are directed towards vacancies. Spatial correlations between successive jumps, which are accounted for by KMC but ignored by MFT, tend to make $D_s(\theta)$ decrease more rapidly than $(1 - \theta)$.¹⁹⁷

It remains challenging in the general case to apply MFT to diffusion in zeolites, especially when considering a heterogeneous lattice with several distinct site types, such as the lattice of cation and window sites for benzene in FAU-type zeolites. To address this issue for diffusion through cage-type zeolites, Saravanan and Auerbach have shown that a mean field analysis of cage-to-cage motion yields $D_s(\theta) \cong \frac{1}{6}k_\theta a_\theta^2$, where a_θ is the mean intercage jump length, and $1/k_\theta$ is the mean cage residence time.¹⁹⁵ Since a_θ has a very weak temperature and loading dependence,²³⁵ e.g. remaining in the range 11–13 Å for FAU-type zeolites, the cage-to-cage rate coefficient carries the interesting T and θ dependencies. Such a formulation is expected to hold for many guests in cage-type zeolites, but not for long chain alkanes ($> C_8$) in FAU-type zeolites, which are dominated by window-to-window jumps rather than by cage-to-cage jumps.⁶⁴

Saravanan and Auerbach have also shown that k_θ is given by $k_\theta = \kappa \cdot k_1 \cdot P_1$, where P_1 is the probability of occupying a window site between adjacent cages, k_1 is the total rate of leaving a window site, and κ is the transmission coefficient for cage-to-cage motion.¹⁹⁵ This theory provides a picture of cage-to-cage motion involving transition state theory ($k_1 \cdot P_1$) with dynamical corrections (κ). Saravanan and Auerbach have found that P_1 increases with loading when cage sites are more stable than window sites, that k_1 decreases with loading in all cases, and that the balance between k_1 and P_1 controls the loading dependence of self diffusion. Below we discuss applications of this theory to benzene in FAU-type zeolites.^{227,203}

2. Fickian vs. Maxwell-Stefan Theory

Two theoretical formulations exist for modeling non-equilibrium diffusion, hereafter denoted “transport diffusion,” which ultimately arises from a chemical potential gradient or similar driving force.^{8,9} The formulation developed by Fick involves linear response theory relating macroscopic particle flows to concentration gradients, according to $J = -D\nabla\theta$, where J is the net particle flux through a surface \mathcal{S} , D is the transport diffusivity, and $\nabla\theta$ is the local concentration gradient perpendicular to the surface \mathcal{S} .¹⁵⁵ While this perspective is conceptually simple, it breaks down qualitatively in remarkably simple cases, such as a closed system consisting of a liquid in contact with its equilibrium vapor. In this case, Fick’s law would predict a non-zero macroscopic flux; none exists because the chemical potential gradient vanishes at equilibrium. Fick’s law can be generalized to treat very simple multicomponent systems,^{16,200,242,244–246} such as co-diffusion and counter-diffusion of identical, tagged particles.

Despite these shortcomings, Fick’s law remains the most natural formulation for transport diffusion through Langmuirian lattice models of zeolite-guest systems. These involve regular lattices of identical sorption sites where guest-guest interactions are ignored, except for exclusion of multiple site occupancy. Such model systems exhibit Langmuir adsorption isotherms, and give single-component transport diffusivities that are independent of loading.²⁴⁷ Moreover, for such systems the equation $J = -D\nabla\theta$ is exact for all concentration gradients, i.e. all higher order terms beyond linear response theory cancel. Nelson and Auerbach exploit this fact in their lattice model studies of counter-permeation through anisotropic²⁰⁰ and single-file nanoporous membranes,¹⁶ described above in section III B 4.

The other formulation of transport diffusion was developed independently by Maxwell

and Stefan, and begins with the equation $J = -L\nabla\mu$, where L is the so-called Onsager coefficient and $\nabla\mu$ is a local chemical potential gradient at the surface \mathcal{S} .^{8,111} To make contact with other diffusion theories, the Onsager coefficient is written in terms of the so-called corrected diffusivity, D_c , according to $L = \theta D_c/k_B T$, where θ is the local intracrystalline loading at the surface \mathcal{S} . Clearly this formulation does not suffer from the qualitative shortcomings of Fick’s law, and can be properly generalized for complex multicomponent systems.²⁴⁸ The corrected diffusivity depends strongly upon loading for Langmuirian systems, where jump diffusion holds, but depends very weakly on loading for more fluid-like diffusion systems,¹¹¹ making the Maxwell-Stefan formulation more natural for weakly binding zeolite-guest systems. The relationship between the Fickian and Maxwell-Stefan diffusivities is often called the Darken equation, given by:⁸

$$D = D_c \left(\frac{\partial \ln f}{\partial \ln \theta} \right)_T, \quad (3.8)$$

where f is the fugacity of the external fluid phase. Other versions of the Darken equation often appear, e.g., where D_c is replaced with D_s , the self diffusivity.

3. Recent Applications

Finite Loadings. MFT has been used to explore how site connectivity influences spatial correlations,¹⁹⁷ how site energetics control loading dependencies,²⁰⁴ and how system size controls tracer exchange residence times,²⁴³ as discussed above in the context of comparable KMC simulations. Saravanan *et al.* applied MFT in conjunction with the parabolic jump model to obtain analytical expressions for the cage-to-cage rate constant k_θ , as a function of chemical potential and temperature for the specific example of benzene in FAU-type zeolites.^{203,227} Saravanan *et al.* considered two levels of guest-guest interaction: (i) site blocking alone and (ii) site blocking with nearest neighbor guest-guest attractions. In what follows, the window and cation sites for benzene in FAU-type zeolites are denoted sites 1 and 2, respectively.

In this site blocking model, there are only four fundamental rate constants in the problem, $\{k_{i \rightarrow j}\}$, where $i, j = 1, 2$. For example, the rate constant $k_{2 \rightarrow 1}$ is the fundamental rate constant for jumping from a cation site to a window site (see figure 4). In the limit where cation sites are very stable compared to window sites, which models benzene in Na-Y, these MFT equations reduce to:¹⁹⁵

$$k_\theta \cong \frac{3}{2} \left(\frac{2}{2 - 3\theta} \cdot \frac{k_{1 \rightarrow 1}}{k_{1 \rightarrow 2}} + 1 \right) k_{2 \rightarrow 1} \quad \text{for } \theta < \frac{2}{3}$$

$$\cong 3(1 - \theta) \left(\frac{3\theta - 2}{\theta} \right) k_{1 \rightarrow 1} \quad \text{for } \theta > \frac{2}{3}. \quad (3.9)$$

These MFT formulas agree well with the results of KMC simulations using input rates calculated for benzene in Na-Y.²²³ For $T \lesssim 650$ K, equations 3.9 give diffusion isotherms consistent with Kärger and Pfeifer’s type IV diffusion isotherm,²³⁴ because jumping out of

Na-Y window sites is much faster than jumping off cations, i.e. $k_{1\rightarrow 1} \gg k_{2\rightarrow 1}$. The type IV isotherm involves a broadly increasing diffusivity at low loadings (as cation sites become occupied), followed by a sharply decreasing diffusivity at high loadings (as all sites become occupied). At present there is a paucity of reliable self-diffusion data for benzene in Na-Y due to the fact that Na-Y crystallites are typically rather small, making intracrystalline diffusion measurements rather challenging. However, QENS data collected at 2 and 4.5 benzenes per cage are consistent with a type I isotherm for benzene in Na-Y,⁴⁵ which is monotonically decreasing.

Saravanan and Auerbach explored the performance of this MFT in the more general case, for arbitrary guest-guest attractions and for arbitrary cation and window stabilities.²⁰³ It should not be surprising that this lattice model of benzene in FAU-type zeolites with guest-guest attractions supports phase transitions from low to high sorbate density, analogous to vapor-liquid equilibrium of bulk benzene.^{206,207} For benzene in Na-X, which involves window sites that are more stable than those in Na-Y, MFT predicts a very broad coexistence region in θ , much broader than that predicted by grand canonical MC simulations.^{206,207} This renders MFT pretty useless for benzene in Na-X, because MFT cannot be used to evaluate diffusivities for the wide range of fractional loadings in the MFT coexistence region. On the other hand, MFT predicts a much narrower coexistence curve for benzene in Na-Y, which increases the range of fractional loadings for which MFT can be evaluated. For these values of θ , MFT gives excellent agreement with KMC simulations of benzene in Na-Y. Even with this more sophisticated treatment of benzene in Na-Y, including guest-guest attractions, we still predict²⁰³ a Kärger and Pfeifer type IV diffusion isotherm.²³⁴ Resolving this discrepancy between theory and QENS may require collecting QENS data at more loadings, and may also require more sophisticated simulation approaches.

Lattice Topology. The diffusion theory discussed above relies on the tetrahedral topology of FAU-type zeolites. Developing such a theory for general frameworks remains challenging. Braun and Sholl developed a Laplace-Fourier transformation method for calculating exact self-diffusion tensors in generalized lattice gas models.¹⁹³ These methods generally involve quite heavy matrix algebra, which can sometimes hide the underlying physical meaning of the parameters. Jousse, Auerbach and Vercauteren developed an alternative method for deriving analytical self-diffusion coefficients at infinite dilution for general lattices, by partitioning the trajectory of a tracer into uncorrelated sequences of jumps.¹²⁵ This approach can be used to analyze both geometric correlations due to the non-symmetric nature of adsorption sites in zeolite pores, and kinetic correlations arising from insufficient thermalization of a molecule in its final site. This method was applied to benzene diffusion in Na-Y (geometric correlations) and to ethane diffusion in silicalite-1 (geometric and kinetic correlations), yielding quantitative agreement with KMC simulations.¹²⁵ The new method was also extended to finite loadings using MFT, yielding a completely analytical approach for modeling diffusion in any guest-zeolite system.

Maxwell-Stefan and Fick. Krishna and van den Broeke modeled the transient permeation fluxes of methane and n-butane through a silicalite-1 membrane using both the Fick and Maxwell-Stefan formulations.²⁴⁹ Transient experiments showed that initially the permeation flux of methane is higher than that of n-butane, but that this methane flux eventually reduces to a lower steady-state value. The Maxwell-Stefan formulation succeeded in reproducing this non-monotonic evolution to steady state for methane; the Fick formulation

failed qualitatively in this regard. This is attributed to the fact that multicomponent systems pose a challenge to the Fick formulation of diffusion. van de Graaf, Kapteijn and Moulijn used the Maxwell-Stefan formulation to interpret permselectivity data for the separations of ethane/methane and propane/methane mixtures with a silicalite-I membrane.²⁵⁰ Based only on separately determined single-component adsorption and diffusion parameters, the Maxwell-Stefan model gave permselectivities in excellent agreement with their experimental data.

As discussed in section IIIB 4, Chen *et al.* augmented the standard diffusion equation (Fick’s second law)⁸ with terms representing the effects of static charge disorder.⁴⁸ They analyzed the resulting equation in the hydrodynamic limit using renormalization group theory,¹⁵⁵ finding that such disorder can diminish self diffusivities in zeolites by one to two orders of magnitude. Nelson, Tsapatsis and Auerbach computed steady-state solutions of the diffusion equation to evaluate the influence of defects, voids and diffusion anisotropy on permeation fluxes through model zeolite membranes.²⁵¹ Nelson *et al.* augmented the lattice configuration shown in figure 8 with various kinds of defect structures, and used a time-dependent, numerical finite difference approach for computing steady-state fluxes in a variety of situations. They found that with a reasonable anisotropy and with a moderate density of voids in the membrane, permeation fluxes can be controlled by jumps perpendicular to the transmembrane direction. This suggests that oriented zeolite membranes may not behave with the intended orientation if there is a sufficient density of defects in the membrane.

IV. CONCLUDING REMARKS

In this review we have explored recent efforts to model the dynamics of sorbed molecules in zeolites with either atomistic methods or lattice models. We assessed recent approaches for constructing guest-zeolite forcefields, as well as atomistic models of aluminosilicate frameworks with charge-compensating cations. We then detailed the techniques and applications of equilibrium molecular dynamics (MD), transition-state theory and reactive flux MD to sorbed molecules in zeolites. Changing focus from atomistic methods to lattice models, we discussed the assumptions underlying such lattice models, and analyzed their validity for molecules in zeolites. We then described the techniques and applications of kinetic Monte Carlo, mean field theory and other continuum theories to modeling transport in complex guest-zeolite systems.

Over the last several years a wealth of insight has been gained from studies modeling dynamics in zeolites. Here we summarize some (but not all) of the key ideas that have recently emerged. A useful picture has developed that relates guest size and shape, and zeolite pore size and topology, to the resulting transport properties of hydrocarbons in all-silica zeolites. We have also gained a better understanding of the role of framework flexibility, especially for molecules in tight-fitting guest-zeolite systems. In general, the analysis of both simulation and experimental data in terms of jump diffusion models has proven very useful for developing simplified pictures of dynamics in zeolites. Regarding dynamics in acidic zeolites, we have learned that the inherent disorder in framework charge and proton distributions can produce cage-to-cage jump rates with significant non-Arrhenius behavior. Furthermore, recent studies have suggested that tunneling dominates proton transfer in

some acidic zeolites at ambient temperatures, and that true proton transfer barriers are being underestimated by neglecting tunneling in the interpretation of experimental mobility data.

Recent simulations on lattice models have provided qualitative insights regarding the relationship between fundamental site-to-site jump rates and the resulting loading dependencies of diffusion. Various loading dependencies have also been connected with subcritical and supercritical states of the confined fluid. For the specific example of benzene in Na-X, recent results point towards the validity of the decreasing loading dependence observed by PFG NMR, while the TZLC data remain mysteriously reproducible. At the same time, a possible discrepancy between simulation and experiment may be emerging for the loading dependence of benzene diffusion in Na-Y. Both atomistic methods and lattice models have contributed to our basic understanding of single-file diffusion in zeolites. In particular, we understand more clearly when to expect anomalous mean square displacements in both simulations and experiments. Finally, while most studies model diffusion in zeolites (translational dynamics), a new emphasis on modeling orientational dynamics has emerged, to reveal more subtle aspects of zeolite structure including possibly Al distributions.

Despite this impressive progress many challenges lay ahead; below we list some desiderata for future modeling of dynamics in zeolites. To begin, we need better representations of charge disorder, as well as other defect structures in zeolites, to determine their impact on diffusion. In parallel, we require better understanding of the external surfaces of zeolite crystallites, to facilitate realistic grand canonical MD simulations of permeation through zeolites. To facilitate modeling in general, more portable forcefields and more tractable *ab initio* MD would allow simultaneous modeling of diffusion and reaction. We seek more realistic lattice models to bridge the gap between atomistic methods and lattice dynamics,¹⁶⁵ to test the presently oversimplified lattice treatments of the loading dependence of activated diffusion. Finally, we hope to understand the loading dependencies of multicomponent diffusion in zeolites, as well as the practical impact of single-file diffusion in zeolite applications.²⁵²

We hope that these computational studies can assist in the design of new materials with advanced performance by elucidating the microscopic factors that control dynamics in zeolites. While this dream is not yet an everyday reality, examples exist today that have the flavor of rational design.²⁵³ We believe that such design will become much more commonplace within the next ten years, with the advent of better algorithms and faster computers. Perhaps even more significant is the need for enhanced cooperation between experiment and simulation, to inspire the next generation of dynamics models for molecules in zeolites.

ACKNOWLEDGMENTS

S.M.A. gratefully acknowledges his research group and collaborators for their invaluable contributions and for many stimulating discussions. This work was supported by the University of Massachusetts at Amherst Faculty Research Grant Program, the Petroleum Research Fund (ACS-PRF 30853-G5), the National Science Foundation (CHE-9403159, CHE-9625735, CHE-9616019 and CTS-9734153), a Sloan Foundation Research Fellowship (BR-3844), a

Camille Dreyfus Teacher-Scholar Award (TC-99-041), the National Environmental Technology Institute, and Molecular Simulations, Inc.

F.J. wishes to thank particularly Prof. D. P. Vercauteren, Director of the Laboratoire de Physico-Chimie Informatique at the University of Namur, for his continuous support, and Prof. A. Lucas, Director of the PAI 4–10, for the attribution of a post-doctoral fellowship. F.J. also acknowledges the FUNDP for the use of the Namur Scientific Computing Facility Center (SCF), and financial support from the FNRS-FRFC, the “Loterie Nationale” for the convention no. 9.4595.96, and IBM Belgium for the Academic Joint Study on “Cooperative Processing for Theoretical Physics and Chemistry.”

REFERENCES

- ¹ D. W. Breck, *Zeolite Molecular Sieves: Structure, Chemistry and Use*, Wiley, New York, 1974.
- ² R. M. Barrer, *Zeolites and Clay Minerals as Sorbents and Molecular Sieves*, Academic Press, London, 1978.
- ³ H. van Bekkum, E. M. Flanigen, and J. C. Jansen, editors, *Introduction to Zeolite Science and Practice*, Elsevier, Amsterdam, 1991.
- ⁴ W. M. Meier and D. H. Olson, *Atlas of Zeolite Structure Types, Third Revised Edition*, Butterworth-Heinemann, London, 1992.
- ⁵ *InsightII 4.0.0 User Guide*, MSI, San Diego, 1996.
- ⁶ B. Herreros, (1996), <http://suzy.unl.edu/Bruno/zeodat/zeodat.html>.
- ⁷ J. Weitkamp, in *Catalysis and Adsorption by Zeolites*, edited by G. Olmann, J. C. Vedrine, and P. A. Jacobs, page 21, Elsevier, Amsterdam, 1991.
- ⁸ J. Kärger and D. M. Ruthven, *Diffusion in Zeolites and Other Microporous Solids*, John Wiley & Sons, New York, 1992.
- ⁹ N. Y. Chen, T. F. Degnan, Jr., and C. M. Smith, *Molecular Transport and Reaction in Zeolites*, VCH Publishers, New York, 1994.
- ¹⁰ D. E. Favre, D. J. Schaefer, S. M. Auerbach, and B. F. Chmelka, *Phys. Rev. Lett.* **81**, 5852 (1998).
- ¹¹ J. Caro, M. Bülow, W. Schirmer, J. Kärger, W. Heink, H. Pfeifer, and S. P. Ždanov, *J. Chem. Soc., Faraday Trans. I* **81**, 2541 (1985).
- ¹² C. R. A. Catlow, editor, *Modelling of Structure and Reactivity in Zeolites*, Academic Press, London, 1992.
- ¹³ P. Demontis and G. B. Suffritti, *Chem. Rev.* **97**, 2845 (1997), and references therein.
- ¹⁴ M. W. Deem, *AIChE J.* **44**, 2569 (1998).
- ¹⁵ S. M. Auerbach, *Int. Rev. Phys. Chem.* **19**, 155 (2000).
- ¹⁶ P. H. Nelson and S. M. Auerbach, *J. Chem. Phys.* **110**, 9235 (1999).
- ¹⁷ E. B. Webb, III and G. S. Grest, *Catal. Letters* **56**, 95 (1998).
- ¹⁸ S. M. Auerbach, L. M. Bull, N. J. Henson, H. I. Metiu, and A. K. Cheetham, *J. Phys. Chem.* **100**, 5923 (1996).
- ¹⁹ C. Hansenne, F. Jousse, L. Leherte, and D. P. Vercauteren, *J. Mol. Cat. A: Chemical* (2000), in press.
- ²⁰ W. Heink, J. Kärger, H. Pfeifer, K. P. Datema, and A. K. Nowak, *J. Chem. Soc., Faraday Trans.* **88**, 3505 (1992).
- ²¹ F. Jousse and E. Cohen De Lara, *J. Phys. Chem.* **100**, 233 (1996).
- ²² D. E. Akporiaye, I. M. Dahl, H. B. Mostad, and R. Wendelbo, *J. Phys. Chem.* **100**, 4148 (1996).
- ²³ D. Ding, B. Li, P. Sun, Q. Jin, and J. Wang, *Zeolites* **15**, 569 (1995).
- ²⁴ A. J. Vega, *J. Phys. Chem.* **100**, 833 (1996).
- ²⁵ C. P. Herrero and R. Ramírez, *J. Phys. Chem.* **96**, 2246 (1992).
- ²⁶ C. P. Herrero, *J. Phys. Chem.* **95**, 3282 (1991).
- ²⁷ J. Klinowski, S. Ramdas, J. M. Thomas, C. A. Fyfe, and J. S. Hartman, *J. Chem. Soc., Faraday Trans. 2* **78**, 1025 (1982).

- ²⁸ E. J. P. Feijen, J. L. Lievens, J. A. Martens, P. J. Grobet, and P. A. Jacobs, *J. Phys. Chem.* **100**, 4970 (1996).
- ²⁹ J. M. Newsam, *J. Phys. Chem.* **93**, 7689 (1989).
- ³⁰ C. F. Mellot, A. M. Davidson, J. Eckert, and A. K. Cheetham, *J. Phys. Chem. B* **102**, 2530 (1998).
- ³¹ C. F. Mellot, A. K. Cheetham, S. Harms, S. Savitz, R. J. Gorte, A. L. Myers, *J. Am. Chem. Soc.* **120**, 5788 (1998).
- ³² G. Vitale, C. F. Mellot, L. M. Bull, and A. K. Cheetham, *J. Phys. Chem. B* **101**, 4559 (1997).
- ³³ D. A. Faux, *J. Phys. Chem. B* **102**, 10658 (1998).
- ³⁴ F. Jousse, S. M. Auerbach, and D. P. Vercauteren, *J. Phys. Chem. B* **104**, 2360 (2000).
- ³⁵ P. Santikary and S. Yashonath, *J. Phys. Chem.* **98**, 9252 (1994).
- ³⁶ S. M. Auerbach, N. J. Henson, A. K. Cheetham, and H. I. Metiu, *J. Phys. Chem.* **99**, 10600 (1995).
- ³⁷ F. Jousse and S. M. Auerbach, *J. Chem. Phys.* **107**, 9629 (1997).
- ³⁸ N. J. Henson, A. K. Cheetham, A. Redondo, S. M. Levine, and J. M. Newsam, Computer simulations of benzene in faujasite-type zeolites, in *Zeolites and Related Microporous Materials: State of the Art 1994*, edited by J. Weitkamp, H. G. Karge, H. Pfeifer, and W. Hölderich, pages 2059–2066, Amsterdam, 1994, Elsevier.
- ³⁹ S. M. Auerbach and H. I. Metiu, *J. Chem. Phys.* **106**, 2893 (1997).
- ⁴⁰ L. Forni and C. F. Viscardi, *J. Catal.* **97**, 480 (1986).
- ⁴¹ M. Bülow, W. Mietk, P. Struve, and P. Lorenz, *J. Chem. Soc., Faraday Trans. I* **79**, 2457 (1983).
- ⁴² P. Lorenz, M. Bülow, and J. Kärger, *Izv. Akad. Nauk. SSSR, Ser. Khim.* , 1741 (1980).
- ⁴³ J. A. Sousa-Gonçalves, R. L. Portsmouth, P. Alexander, and L. F. Gladden, *J. Phys. Chem.* **99**, 3317 (1995).
- ⁴⁴ O. Isfort, B. Boddenberg, F. Fujara, and R. Grosse, *Chem. Phys. Lett.* **288**, 71 (1998).
- ⁴⁵ H. Jobic, A. N. Fitch, and J. Combet, (2000), submitted.
- ⁴⁶ R. Burmeister, H. Schwarz, and B. Boddenberg, *Ber. Bunsenges. Phys. Chem.* **93**, 1309 (1989).
- ⁴⁷ L. M. Bull, N. J. Henson, A. K. Cheetham, J. M. Newsam, and S. J. Heyes, *J. Phys. Chem.* **97**, 11776 (1993).
- ⁴⁸ L. Chen, M. Falcioni, and M. W. Deem, *J. Phys. Chem. B* **104** (2000), in press.
- ⁴⁹ E. Jaramillo and S. M. Auerbach, *J. Phys. Chem. B* **103**, 9589 (1999).
- ⁵⁰ J. M. Newsam, C. M. Freeman, A. M. Gorman, and B. Vessal, *Chem. Comm.* **16**, 1945 (1996).
- ⁵¹ P. Demontis, E. S. Fois, G. B. Suffritti, and S. Quartieri, *J. Phys. Chem.* **94**, 4329 (1990).
- ⁵² C. R. A. Catlow, C. M. Freeman, B. Vessal, S. M. Tomlinson, and M. Leslie, *J. Chem. Soc., Faraday Trans.* **87**, 1947 (1991).
- ⁵³ P. Demontis, G. B. Suffritti, E. S. Fois, and S. Quartieri, *J. Phys. Chem.* **96**, 1482 (1992).
- ⁵⁴ K. S. Smirnov, *Chem. Phys. Lett.* **229**, 250 (1994).
- ⁵⁵ A. Bouyermaouen and A. Bellemans, *J. Chem. Phys.* **108**, 2170 (1998).
- ⁵⁶ S. Fritzsche, M. Wolfsberg, R. Haberlandt, P. Demontis, G. P. Suffritti, and A. Tilocca, *Chem. Phys. Lett.* **296**, 253 (1998).
- ⁵⁷ G. Schrimpf, M. Schlenkrich, J. Brickmann, and P. Bopp, *J. Phys. Chem.* **96**, 7404 (1992).

- ⁵⁸ G. Sastre, C. R. A. Catlow, and A. Corma, *J. Phys. Chem. B* **103**, 5187 (1999).
- ⁵⁹ T. Mosell, G. Schrimpf, and J. Brickmann, *J. Phys. Chem. B* **101**, 9476 (1997).
- ⁶⁰ T. Mosell, G. Schrimpf, and J. Brickmann, *J. Phys. Chem. B* **101**, 9485 (1997).
- ⁶¹ F. Jousse, D. P. Vercauteren, and S. M. Auerbach, *J. Phys. Chem. B* (2000), in press.
- ⁶² K. T. Thomson, A. V. McCormick, and H. T. Davis, *J. Chem. Phys.* **112**, 3345 (2000).
- ⁶³ M. Gaub, S. Fritzsche, R. Haberlandt, and D. N. Theodorou, *J. Phys. Chem. B* **103**, 4721 (1999).
- ⁶⁴ L. A. Clark, G. T. Ye, A. Gupta, L. L. Hall, and R. Q. Snurr, *J. Chem. Phys.* **111**, 1209 (1999).
- ⁶⁵ D. S. Sholl and C. K. Lee, *J. Chem. Phys.* **112**, 817 (2000).
- ⁶⁶ D. S. Sholl, *Chem. Phys. Lett.* **305**, 269 (1999).
- ⁶⁷ D. Schuring, A. P. J. Jansen, and R. A. van Santen, *J. Phys. Chem. B* **104**, 941 (2000).
- ⁶⁸ E. B. Webb, III, G. S. Grest, and M. Mondello, *J. Phys. Chem. B* **103**, 4949 (1999).
- ⁶⁹ H. L. Tepper, J. P. Hoogenboom, N. F. A. van der Vegt, and W. J. Briels, *J. Chem. Phys.* **110**, 11511 (1999).
- ⁷⁰ L. N. Gergidis and D. N. Theodorou, *J. Phys. Chem. B* **103**, 3380 (1999).
- ⁷¹ S. Jost, N.-K. Bär, S. Fritzsche, R. Haberlandt, and J. Kärger, *J. Phys. Chem. B* **102**, 6375 (1998).
- ⁷² R. Q. Snurr, A. T. Bell, and D. N. Theodorou, *J. Phys. Chem.* **98**, 11948 (1994).
- ⁷³ T. R. Forester and W. Smith, *J. Chem. Soc., Faraday Trans.* **93**, 3249 (1997).
- ⁷⁴ R. J.-M. Pellenq and D. Nicholson, *J. Phys. Chem.* **98**, 13339 (1994).
- ⁷⁵ D. Nicholson, A. Boutin, and R. J.-M. Pellenq, *Mol. Sim.* **17**, 217 (1996).
- ⁷⁶ A. V. Larin and E. Cohen de Lara, *Mol. Physics* **88**, 1399 (1996).
- ⁷⁷ F. Jousse, A. V. Larin, and E. Cohen De Lara, *J. Phys. Chem.* **100**, 238 (1996).
- ⁷⁸ M. D. Macedonia and E. J. Maginn, *Mol. Physics* **96**, 1375 (1999).
- ⁷⁹ F. Jousse, S. M. Auerbach, H. Jobic, and D. P. Vercauteren, *J. Phys. IV: Proceedings* (2000), in press.
- ⁸⁰ L. N. Gergidis, D. N. Theodorou, and H. Jobic, *J. Phys. Chem. B* **104**, 5541 (2000).
- ⁸¹ V. Lachet, A. Boutin, R. J.-M. Pellenq, D. Nicholson, and A. H. Fuchs, *J. Phys. Chem.* **100**, 9006 (1996).
- ⁸² N. Raj, G. Sastre, and C. R. A. Catlow, *J. Phys. Chem. B* **103**, 11007 (1999).
- ⁸³ G. Sastre, N. Raj, C. R. A. Catlow, R. Roque-Malherbe, and A. Corma, *J. Phys. Chem. B* **102**, 3198 (1998).
- ⁸⁴ P. P. Ewald, *Ann. Physik* **64**, 253 (1921).
- ⁸⁵ M. F. Allen and D. J. Tildesley, *Computer Simulation of Liquids*, Clarendon Press, Oxford, 1987.
- ⁸⁶ L. Greengard and V. Rokhlin, *J. Comp. Phys.* **73**, 325 (1987).
- ⁸⁷ H. G. Petersen, D. Soelvason, J. W. Perram, and E. R. Smith, *J. Chem. Phys.* **101**, 8870 (1994).
- ⁸⁸ D. K. Remler and P. A. Madden, *Mol. Physics* **70**, 921 (1990).
- ⁸⁹ G. Galli and A. Pasquarello, *First-principles molecular dynamics*, pages 261–313, Kluwer Academic, The Netherlands, 1993.
- ⁹⁰ Bolton, Hase, and Peshlerbe, Direct dynamics simulations of reactive systems, in *Modern Methods for Multidimensional Dynamics for Computations in Chemistry*, edited by D. L. Thompson, World Scientific, New York, 1998.

- ⁹¹ R. Car and M. Parrinello, Phys. Rev. Lett. **55**, 2471 (1985).
- ⁹² K. Schwarz, E. Nusterer, and P. E. Blöchl, Catal. Today **50**, 501 (1999).
- ⁹³ E. Fois and A. Gamba, J. Phys. Chem. B **103**, 1794 (1999).
- ⁹⁴ I. Štich, J. D. Gale, K. Terakura, and M. C. Payne, J. Am. Chem. Soc. **121**, 3292 (1999).
- ⁹⁵ E. Nusterer, P. E. Blöchl, and K. Schwarz, Angewandte Chemie **35**, 175 (1996).
- ⁹⁶ E. Nusterer, P. E. Blöchl, and K. Schwarz, Chem. Phys. Lett. **253**, 448 (1996).
- ⁹⁷ Y. Jeanvoine, J. G. Ángyán, G. Kresse, and J. Hafner, J. Phys. Chem. B **102**, 7307 (1998).
- ⁹⁸ R. Shah, M. C. Payne, M.-H. Lee, and J. D. Gale, Science **271**, 1395 (1996).
- ⁹⁹ R. Shah, J. D. Gale, and M. C. Payne, J. Phys. Chem. **100**, 11688 (1996).
- ¹⁰⁰ F. Filippone and F. A. Gianturco, J. Chem. Phys. **111**, 2761 (1999).
- ¹⁰¹ D. Alfè and M. J. Gillan, Phys. Rev. Lett. **81**, 5161 (1998).
- ¹⁰² G. A. de Wijs, G. Kresse, L. Voçadlo, D. Dobson, D. Alfè, M. J. Gillan, and G. D. Price, Nature **392**, 805 (1998).
- ¹⁰³ P. Demontis, G. B. Suffritti, A. Alberti, S. Quartieri, E. S. Fois, and A. Gamba, Gazz. Chim. Ital. **116**, 459 (1986).
- ¹⁰⁴ D. Frenkel and B. Smit, *Understanding Molecular Simulations*, Academic Press, San Diego, 1996.
- ¹⁰⁵ C. J. Mundy, S. Balasubramanian, K. Bogchi, M. E. Tuckerman, and M. L. Klein, Rev. Comp. Chem. **14**, 291 (2000).
- ¹⁰⁶ M. E. Tuckerman and G. J. Martyna, J. Phys. Chem. B **104**, 159 (2000).
- ¹⁰⁷ W. G. Hoover, Physica A **194**, 450 (1993).
- ¹⁰⁸ W. G. Hoover and O. Kum, Mol. Physics **86**, 685 (1995).
- ¹⁰⁹ M. C. Lovallo and M. Tsapatsis, AIChE Journal **42**, 3020 (1996).
- ¹¹⁰ X. Lin, J. L. Falconer, and R. D. Noble, Chem. Mater. **10**, 3716 (1998).
- ¹¹¹ E. J. Maginn, A. T. Bell, and D. N. Theodorou, J. Phys. Chem. **97**, 4173 (1993).
- ¹¹² G. S. Heffelfinger and F. van Swol, J. Chem. Phys. **100**, 7548 (1994).
- ¹¹³ D. Nicholson, Supramolecular Science **5**, 275 (1998).
- ¹¹⁴ K. P. Travis and K. E. Gubbins, Langmuir **15**, 6050 (1999).
- ¹¹⁵ L. Xu, T. T. Tsotsis, and M. Sahimi, J. Chem. Phys. **111**, 3252 (1999).
- ¹¹⁶ I. Wold and B. Hafskjold, Int. J. Thermophys. **20**, 847 (1999).
- ¹¹⁷ K. P. Travis and K. E. Gubbins, J. Chem. Phys. **112**, 1984 (2000).
- ¹¹⁸ L. Xu, M. G. Sedigh, T. T. Tsotsis, and M. Sahimi, J. Chem. Phys. **112**, 910 (2000).
- ¹¹⁹ K. Hahn, J. Kärger, and V. Kukla, Phys. Rev. Lett. **76**, 2762 (1996).
- ¹²⁰ V. Kukla, J. Kornatowski, D. Demuth, I. Girnus, H. Pfeifer, L. V. C. Rees, S. Schunk, K. K. Unger, and J. Kärger, Science **272**, 702 (1996).
- ¹²¹ H. van Beijeren, K. W. Kehr, and R. Kutner, Phys. Rev. B **28**, 5711 (1983).
- ¹²² R. L. June, A. T. Bell, and D. N. Theodorou, J. Phys. Chem. **96**, 1051 (1992).
- ¹²³ F. Jousse, L. Leherte, and D. P. Vercauteren, J. Phys. Chem. B **101**, 4717 (1997).
- ¹²⁴ J. Kärger, P. Demontis, G. B. Suffritti, and A. Tilocca, J. Chem. Phys. **110**, 1163 (1999).
- ¹²⁵ F. Jousse, S. M. Auerbach, and D. P. Vercauteren, J. Chem. Phys. **112**, 1531 (2000).
- ¹²⁶ S. W. Lovesey, *Theory of Neutron Scattering from Condensed Matter Vol. 1: Nuclear Scattering*, Clarendon Press, Oxford, 1984.
- ¹²⁷ H. Jobic, M. Bée, and G. J. Kearley, Zeolites **12**, 146 (1992).
- ¹²⁸ D. Bougeard, C. Brémard, D. Dumont, M. Le Maire, J.-M. Manoli, and C. Potvin, J.

- Phys. Chem. B **102**, 10805 (1998).
- ¹²⁹ R. L. June, A. T. Bell, and D. N. Theodorou, J. Phys. Chem. **94**, 8232 (1990).
- ¹³⁰ A. K. Nowak, C. J. J. den Ouden, S. D. Pickett, B. Smit, A. K. Cheetham, M. F. M. Post, and J. M. Thomas, J. Phys. Chem. **95**, 848 (1991).
- ¹³¹ S. J. Goodbody, K. Watanabe, D. MacGowan, J. P. R. B. Walton, and N. Quirke, J. Chem. Soc., Faraday Trans. **87**, 1951 (1991).
- ¹³² F. Jousse, L. Leherte, and D. P. Vercauteren, J. Mol. Cat. A: Chemical **119**, 165 (1997).
- ¹³³ R. C. Runnebaum and E. J. Maginn, J. Phys. Chem. B **101**, 6394 (1997).
- ¹³⁴ H. Jobic, M. Bée, and J. Caro, Translational mobility of *n*-butane and *n*-hexane in ZSM-5 measured by quasi-elastic neutron scattering, in *Proceedings of the 9th International Zeolite Conference*, edited by R. von Ballmoos et al., pages 121–128, Butterworth-Heinemann, 1993.
- ¹³⁵ J. B. Nicholas, F. R. Trouw, J. E. Mertz, L. E. Iton, and A. F. Hopfinger, J. Phys. Chem. **97**, 4149 (1993).
- ¹³⁶ V. A. Ermoshin and V. Engel, J. Phys. Chem. A **103**, 5116 (1999).
- ¹³⁷ E. Hernández and C. R. A. Catlow, Proc. Roy. Soc. Lond. A **448**, 143 (1995).
- ¹³⁸ E. J. Maginn, A. T. Bell, and D. N. Theodorou, J. Phys. Chem. **100**, 7155 (1996).
- ¹³⁹ V. Lachet, A. Boutin, B. Tavitian, and A. H. Fuchs, Faraday Discuss. **106**, 307 (1997).
- ¹⁴⁰ R. Krishna, B. Smit, and T. J. H. Vlugt, J. Phys. Chem. A **102**, 7727 (1998).
- ¹⁴¹ V. Lachet, A. Boutin, B. Tavitian, and A. H. Fuchs, J. Phys. Chem. B **103**, 9224 (1999).
- ¹⁴² M. D. Macedonia and E. J. Maginn, Grand canonical Monte Carlo simulation of single component and binary mixture adsorption in zeolites, in *Proceedings of the 12th International Zeolite Conference*, pages 363–370, Materials Research Society, 1999.
- ¹⁴³ T. J. H. Vlugt, R. Krishna, and B. Smit, J. Phys. Chem. B **103**, 1102 (1999).
- ¹⁴⁴ D. S. Sholl and K. A. Fichthorn, J. Chem. Phys. **107**, 4384 (1997).
- ¹⁴⁵ P. A. Fedders, Phys. Rev. B **17**, 40 (1978).
- ¹⁴⁶ J. Kärger and H. Pfeifer, Diffusion anisotropy and single-file diffusion in zeolites, in *Proc. 9th Int. Zeolite Conf., Montreal 1992*, edited by R. von Ballmoos et al., pages 129–136, Butterworth-Heinemann, 1993.
- ¹⁴⁷ V. Kukla, K. Hahn, J. Kärger, J. Kornatowski, and H. Pfeifer, Anomalous diffusion in AlPO₄-5, in *Proceedings of the 2nd Polish-German Zeolite Colloquium*, edited by M. Rozwadowski, pages 110–119, Toruń, Poland, 1995, Nicholas Copernicus University Press.
- ¹⁴⁸ C. Rödenbeck, J. Kärger, and K. Hahn, J. Catal. **157**, 656 (1995).
- ¹⁴⁹ G. D. Lei, B. T. Carvill, and W. M. H. Sachtler, Applied Cat. A: General **142**, 347 (1996).
- ¹⁵⁰ D. Keffer, A. V. McCormick, and H. T. Davis, Mol. Phys. **87**, 367 (1996).
- ¹⁵¹ K. Hahn and J. Kärger, J. Phys. Chem. **100**, 316 (1996).
- ¹⁵² D. S. Sholl and K. A. Fichthorn, Phys. Rev. Lett. **79**, 3569 (1997).
- ¹⁵³ R. L. June, A. T. Bell, and D. N. Theodorou, J. Phys. Chem. **95**, 8866 (1991).
- ¹⁵⁴ D. Chandler, J. Chem. Phys. **68**, 2959 (1978).
- ¹⁵⁵ D. Chandler, *Introduction to Modern Statistical Mechanics*, Oxford University Press, New York, 1987.
- ¹⁵⁶ P. Pechukas, Transition state theory, in *Dynamics of Molecular Collisions*, edited by W. Miller, page 269, Plenum, New York, 1976.
- ¹⁵⁷ W. H. Miller, J. Chem. Phys. **61**, 1823 (1974).

- ¹⁵⁸ A. F. Voter and J. D. Doll, *J. Chem. Phys.* **82**, 80 (1985).
- ¹⁵⁹ G. A. Voth, D. Chandler, and W. H. Miller, *J. Chem. Phys.* **91**, 7749 (1989).
- ¹⁶⁰ A. Voter, *J. Chem. Phys.* **82**, 1890 (1985).
- ¹⁶¹ G. H. Vineyard, *J. Phys. Chem. Solids* **3**, 121 (1957).
- ¹⁶² T. P. Straatsma, *Rev. in Comp. Chem.* **9** (1996).
- ¹⁶³ E. M. Sevick, A. T. Bell, and D. N. Theodorou, *J. Chem. Phys.* **98**, 3196 (1993).
- ¹⁶⁴ H. Jonsson, G. Mills, and K. W. Jacobsen, Nudged elastic band method for finding minimum energy paths of transitions, in *Classical and Quantum Dynamics in Condensed Phase Simulations*, edited by B. J. Berne, G. Ciccotti, and D. F. Coker, page 385, World Scientific, 1998.
- ¹⁶⁵ A. Voter, *J. Chem. Phys.* **106**, 4665 (1997).
- ¹⁶⁶ C. Dellago, P. G. Bolhuis, F. S. Csajka, and D. Chandler, *J. Chem. Phys.* **108**, 1964 (1998).
- ¹⁶⁷ J. Kärgler, *J. Phys. Chem.* **95**, 5558 (1991).
- ¹⁶⁸ F. Jousse, S. M. Auerbach, and D. P. Vercauteren, *J. Phys. Chem. B* **102**, 6507 (1998).
- ¹⁶⁹ T. Mosell, G. Schrimpf, C. Hahn, and J. Brickmann, *J. Phys. Chem.* **100**, 4571 (1996).
- ¹⁷⁰ T. Mosell, G. Schrimpf, and J. Brickmann, *J. Phys. Chem.* **100**, 4582 (1996).
- ¹⁷¹ C. Tunca and D. M. Ford, *J. Chem. Phys.* **111**, 2751 (1999).
- ¹⁷² B. Bigot and V. H. Peuch, *J. Phys. Chem. B* **102**, 8696 (1998).
- ¹⁷³ D. S. Sholl, *Chem. Eng. J.* **74**, 25 (1999).
- ¹⁷⁴ M. J. Murphy, G. A. Voth, and A. L. R. Bug, *J. Phys. Chem. B* **101**, 491 (1997).
- ¹⁷⁵ T. N. Truong, *J. Phys. Chem. B* **101**, 2750 (1997).
- ¹⁷⁶ Q. Wang, S. R. Challa, D. S. Sholl, and J. K. Johnson, *Phys. Rev. Lett.* **82**, 956 (1999).
- ¹⁷⁷ J. T. Fermann and S. M. Auerbach, *J. Chem. Phys.* **112**, 6787 (2000).
- ¹⁷⁸ J. T. Fermann, C. Blanco, and S. M. Auerbach, *J. Chem. Phys.* **112**, 6779 (2000).
- ¹⁷⁹ J. Sauer, M. Sierka, and F. Haase, in *Transition State Modeling for Catalysis*, edited by D. G. Truhlar and K. Morokuma, number 721 in ACS Symposium Series, chapter 28, pages 358–367, ACS, Washington, 1999.
- ¹⁸⁰ M. Sierka and J. Sauer, *J. Chem. Phys.* **112**, 6983 (2000).
- ¹⁸¹ R. Hernandez and W. H. Miller, *Chem. Phys. Lett.* **214**, 129 (1993).
- ¹⁸² E. Ising, *Z. Phys* **31**, 253 (1925).
- ¹⁸³ R. Gomer, *Rep. Prog. Phys.* **53**, 917 (1990).
- ¹⁸⁴ A. Z. Panagiotopoulos, *J. Chem. Phys.* **112**, 7132 (2000).
- ¹⁸⁵ N. G. van Kampen, *Stochastic Processes in Physics and Chemistry*, North Holland Publishing Company, New York, 1981.
- ¹⁸⁶ C. Blanco, C. Saravanan, M. Allen, and S. M. Auerbach, *J. Chem. Phys.* (2000), submitted.
- ¹⁸⁷ J. Jacobsen, K. W. Jacobsen, and J. P. Sethna, *Phys. Rev. Lett.* **79**, 2843 (1997).
- ¹⁸⁸ K. D. Dobbs and D. J. Doren, *J. Chem. Phys.* **97**, 3722 (1992).
- ¹⁸⁹ D. Cowell Senft and G. Ehrlich, *Phys. Rev. Lett.* **74**, 294 (1995).
- ¹⁹⁰ T. R. Linderoth, S. Horch, E. Lægsgaard, I. Stensgaard, and F. Besenbacher, *Phys. Rev. Lett.* **78**, 4978 (1997).
- ¹⁹¹ E. Hershkovitz, P. Talkner, E. Pollak, and Y. Geogievskii, *Surf. Sci.* **421**, 73 (1999).
- ¹⁹² Z. Y. Zhang, K. Haug, and H. I. Metiu, *J. Chem. Phys.* **93**, 3614 (1990).
- ¹⁹³ O. M. Braun and C. A. Sholl, *Phys. Rev. B* **58**, 14870 (1998).

- ¹⁹⁴ M. W. Deem, J. M. Newsam, and J. A. Creighton, *J. Am. Chem. Soc.* **114**, 7198 (1992).
- ¹⁹⁵ C. Saravanan and S. M. Auerbach, *J. Chem. Phys.* **107**, 8120 (1997).
- ¹⁹⁶ M. C. Mitchell, A. V. McCormick, and H. T. Davis, *Z. Phys. B* **97**, 353 (1995).
- ¹⁹⁷ M. O. Coppens, A. T. Bell, and A. K. Chakraborty, *Chem. Eng. Sci.* **53**, 2053 (1998).
- ¹⁹⁸ S. Y. Bhide and S. Yashonath, *J. Chem. Phys.* **111**, 1658 (1999).
- ¹⁹⁹ S. Y. Bhide and S. Yashonath, *J. Phys. Chem. B* **104**, 2607 (2000).
- ²⁰⁰ P. H. Nelson and S. M. Auerbach, *Chem. Eng. J.* **74**, 43 (1999).
- ²⁰¹ P. H. Nelson, A. B. Kaiser, and D. M. Bibby, *J. Catal.* **127**, 101 (1991).
- ²⁰² D. Keffer, A. V. McCormick, and H. T. Davis, *J. Phys. Chem.* **100**, 967 (1996).
- ²⁰³ C. Saravanan and S. M. Auerbach, *J. Chem. Phys.* **110**, 11000 (1999).
- ²⁰⁴ M. O. Coppens, A. T. Bell, and A. K. Chakraborty, *Chem. Eng. Sci.* **54**, 3455 (1999).
- ²⁰⁵ B. L. Trout, A. K. Chakraborty, and A. T. Bell, *Chem. Eng. Sci.* **52**, 2265 (1997).
- ²⁰⁶ C. Saravanan and S. M. Auerbach, *J. Chem. Phys.* **109**, 8755 (1998).
- ²⁰⁷ I. Dukovski, C. Saravanan, J. Machta, and S. M. Auerbach, *J. Chem. Phys.* (2000), in press.
- ²⁰⁸ J. Kärger, Single-file diffusion in zeolites, in *Molecular Sieves - Science and Technology Vol. 7: Sorption and Diffusion*, edited by H. G. Karge and J. Weitkamp, Springer-Verlag, Berlin, New York, 1999, and references therein.
- ²⁰⁹ D. N. Theodorou and J. Wei, *J. Catal.* **83**, 205 (1983).
- ²¹⁰ L. F. Gladden, J. A. Sousa-Gonçalves, and P. Alexander, *J. Phys. Chem. B* **101**, 10121 (1997).
- ²¹¹ K. A. Fichtorn and W. H. Weinberg, *J. Chem. Phys.* **95**, 1090 (1991).
- ²¹² H. I. Metiu, Y. T. Lu, and Z. Y. Zhang, *Science* **255**, 1088 (1992).
- ²¹³ C. Saravanan, PhD thesis, University of Massachusetts at Amherst, 1999.
- ²¹⁴ P. Maksym, *Semicond. Sci. Technol.* **3**, 594 (1988).
- ²¹⁵ R. Krishna, T. J. H. Vlugt, and B. Smit, *Chem. Eng. Sci.* **54**, 1751 (1999).
- ²¹⁶ L. F. Gladden, M. Hargreaves, and P. Alexander, *Chem. Eng. J.* **74**, 57 (1999).
- ²¹⁷ R. M. Barrer, *J. Chem. Soc., Faraday Trans.* **86**, 1123 (1990).
- ²¹⁸ D. M. Ford and E. D. Glandt, *J. Phys. Chem.* **99**, 11543 (1995).
- ²¹⁹ D. M. Ford and E. D. Glandt, *J. Membrane Sci.* **107**, 47 (1995).
- ²²⁰ K. Schmidt-Rohr and H. W. Spiess, *Multidimensional Solid-State NMR and Polymers*, Academic Press, London, 1994.
- ²²¹ B. Boddenberg and B. Beerwerth, *J. Phys. Chem.* **93**, 1440 (1989).
- ²²² D. J. Schaefer, D. E. Favre, M. Wilhelm, S. J. Weigel, and B. F. Chmelka, *J. Am. Chem. Soc.* **119**, 9252 (1997).
- ²²³ C. Saravanan and S. M. Auerbach, *J. Chem. Phys.* **107**, 8132 (1997).
- ²²⁴ R. Q. Snurr, *Chem. Eng. J.* **74** (1999).
- ²²⁵ I. Kuscer and J. J. M. Beenakker, *J. Stat. Phys.* **87**, 1083 (1997).
- ²²⁶ C. Rodenbeck, J. Kärger, and K. Hahn, *Phys. Rev. E* **55**, 5697 (1997).
- ²²⁷ C. Saravanan, F. Jousse, and S. M. Auerbach, *Phys. Rev. Lett.* **80**, 5754 (1998).
- ²²⁸ M. Bülow, U. Härtel, U. Müller, and K. K. Unger, *Ber. Bunsen-Ges. Phys. Chem.* **94**, 74 (1990).
- ²²⁹ D. Shen and L. V. C. Rees, *J. Chem. Soc., Faraday Trans.* **86**, 3687 (1990).
- ²³⁰ P. R. van Tassel, S. A. Somers, H. T. Davis, and A. V. McCormick, *Chem. Eng. Sci.* **49**, 2979 (1994).

- ²³¹ P. H. Nelson, A. B. Kaiser, and D. M. Bibby, *Zeolites* **11**, 337 (1991).
- ²³² P. H. Nelson and D. M. Bibby, *Stud. Surf. Sci. Catal.* **68**, 407 (1991).
- ²³³ D. Stauffer and A. Aharony, *Introduction to Percolation Theory*, Taylor & Francis, Inc., Bristol, PA, 1991.
- ²³⁴ J. Kärger and H. Pfeifer, *Zeolites* **7**, 90 (1987).
- ²³⁵ C. Saravanan, F. Jousse, and S. M. Auerbach, *J. Chem. Phys.* **108**, 2162 (1998).
- ²³⁶ A. Germanus, J. Kärger, H. Pfeifer, N. N. Samulevic, and S. P. Zdanov, *Zeolites* **5**, 91 (1985).
- ²³⁷ S. Brandani, Z. Xu, and D. Ruthven, *Microporous Materials* **7**, 323 (1996).
- ²³⁸ H. Jobic, M. Bée, J. Kärger, H. Pfeifer, and J. Caro, *J. Chem. Soc., Chem. Commun.* , 341 (1990).
- ²³⁹ D. M. Shen and L. V. C. Rees, *Zeolites* **11**, 666 (1991).
- ²⁴⁰ G. Vitale, L. M. Bull, R. E. Morris, A. K. Cheetham, B. H. Toby, C. G. Coe, and J. E. MacDougall, *J. Phys. Chem.* **99**, 16087 (1995).
- ²⁴¹ B. L. Trout, A. K. Chakraborty, and A. T. Bell, *J. Phys. Chem.* **100**, 17582 (1996).
- ²⁴² P. H. Nelson and J. Wei, *J. Catal.* **136**, 263 (1992).
- ²⁴³ C. Rodenbeck and J. Kärger, *J. Chem. Phys.* **110**, 3970 (1999).
- ²⁴⁴ K. W. Kehr, K. Binder, and S. M. Reulein, *Phys. Rev. B* **39**, 4891 (1989).
- ²⁴⁵ W. R. Qureshi and J. Wei, *J. Catal.* **126**, 126 (1990).
- ²⁴⁶ K. Binder, *Rep. Prog. Phys.* **60**, 487 (1997).
- ²⁴⁷ R. Kutner, *Phys. Lett. A* **81**, 239 (1981).
- ²⁴⁸ R. Krishna, *Chem. Eng. Sci.* **48**, 845 (1993).
- ²⁴⁹ R. Krishna and L. J. P. van den Broeke, *Chem. Eng. J. Biochem. Eng. J.* **57**, 155 (1995).
- ²⁵⁰ J. M. van de Graaf, F. Kapteijn, and J. A. Moulijn, *AIChE J.* **45**, 497 (1999).
- ²⁵¹ P. H. Nelson, M. Tsapatsis, and S. M. Auerbach, *J. Membrane Sci.* (2000), submitted.
- ²⁵² C. Rödenbeck, J. Kärger, and K. Hahn, *J. Catal.* **176**, 513 (1998).
- ²⁵³ C. C. Freyhardt, M. Tsapatsis, R. F. Lobo, K. J. Balkus, M. E. Davis, et al., *Nature* **381**, 295 (1996).

FIGURES

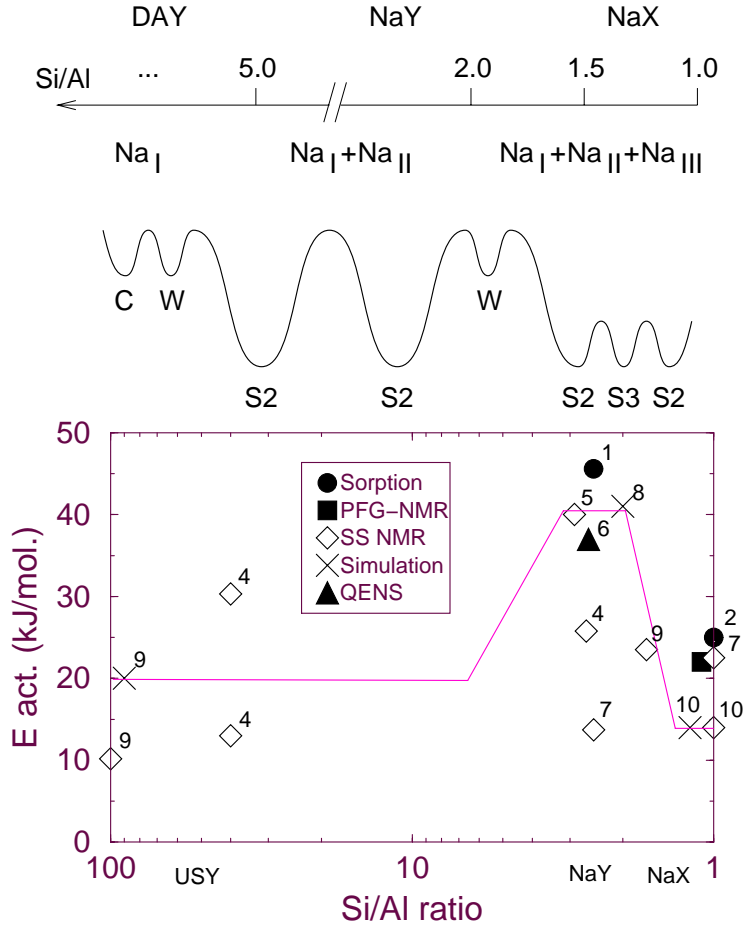


FIG. 1. Activation energies of benzene diffusion in FAU-type zeolites. The top part shows Si:Al ratios of FAU-type zeolites, with the corresponding occupied cation sites. The middle part represents schematic benzene adsorption sites, and the energy barriers between them arising from different cation distributions. C is a benzene supercage site far from a cation, W is a benzene window site far from a cation, S2 is a cage site close to an S_{II} cation, S3 is a window site close to an S_{III} cation. The bottom part gives diffusion activation energies for various Si:Al ratios. The solid line shows the overall trend from simulations, symbols are particular experiment or simulation results: 1. Forni *et al.*,⁴⁰ 2. Bülow *et al.*,⁴¹ 3. Lorenz *et al.*,⁴² 4. Sousa-Gonçalves *et al.*,⁴³ 5. Isfort *et al.*,⁴⁴ 6. Jobic *et al.*,⁴⁵ 7. Burmeister *et al.*,⁴⁶ 8. Auerbach *et al.*,³⁶ 9. Bull *et al.*⁴⁷ and 10. Auerbach *et al.*¹⁸

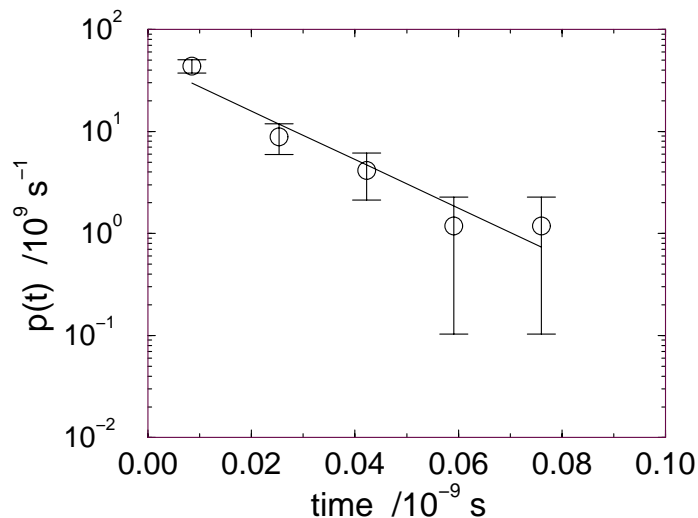


FIG. 2. Cage residence time distribution of benzene in zeolite LTL showing agreement with Poisson statistics, computed from a 1 ns molecular dynamics simulation at 800 K with a single benzene molecule in the simulation cell.

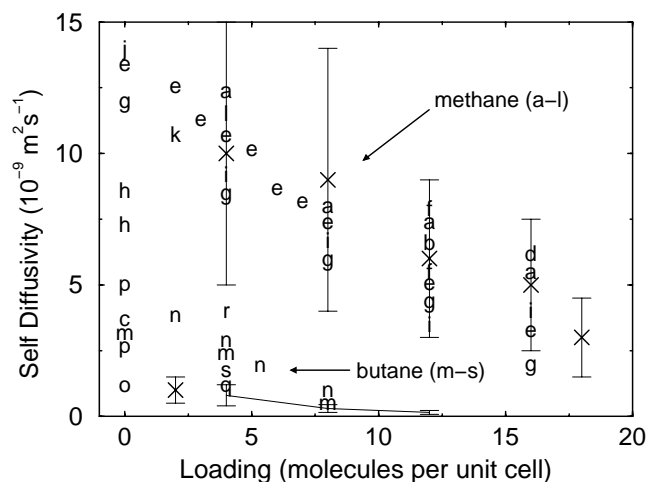


FIG. 3. Self-diffusion isotherms of methane and butane in silicalite-1 at 300K, from PFG NMR, QENS and MD simulations, showing good agreement with the $(1 - \theta)$ loading dependence predicted by mean field theory. Crosses are NMR data from Caro *et al.*¹¹ for methane and Heink *et al.*²⁰ for butane, while the star shows QENS butane data from Jovic *et al.*¹³⁴ In all cases, error bars represent an estimated 50% uncertainty. Letters are MD results (slightly spread for clarity): a–l for methane and m–s for butane, from the following references: (a) June *et al.*,¹²⁹ (b) Demontis *et al.*,⁵¹ (c) Catlow *et al.*,⁵² (e) Goodbody *et al.*,¹³¹ (f) Demontis *et al.*,⁵³ (g) Nicholas *et al.*,¹³⁵ (h) Smirnov,⁵⁴ (i) Jost *et al.*,⁷¹ (j) Ermoshin and Engel,¹³⁶ (k) Schuring *et al.*,⁶⁷ (l) Gergidis and Theodorou,⁷⁰ (m) June *et al.*,¹²² (n) Hernández and Catlow,¹³⁷ (o) Maginn *et al.*,¹³⁸ (p) Bouyermaouen and Bellemans,⁵⁵ (q) Goodbody *et al.*,¹³¹ (r) Gergidis and Theodorou⁷⁰ and (s) Schuring *et al.*⁶⁷

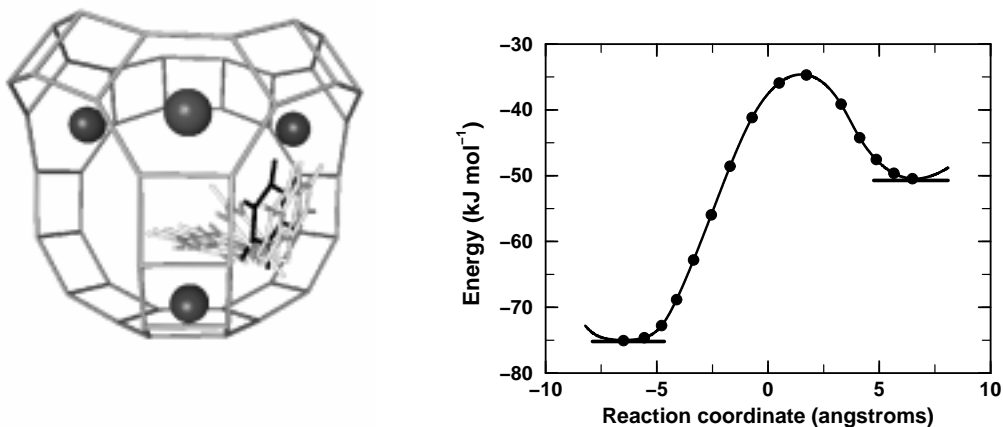


FIG. 4. Cation \leftrightarrow window path for benzene in Na-Y (transition state indicated in bold), with a calculated barrier of 41 kJ mol^{-1} .³⁶

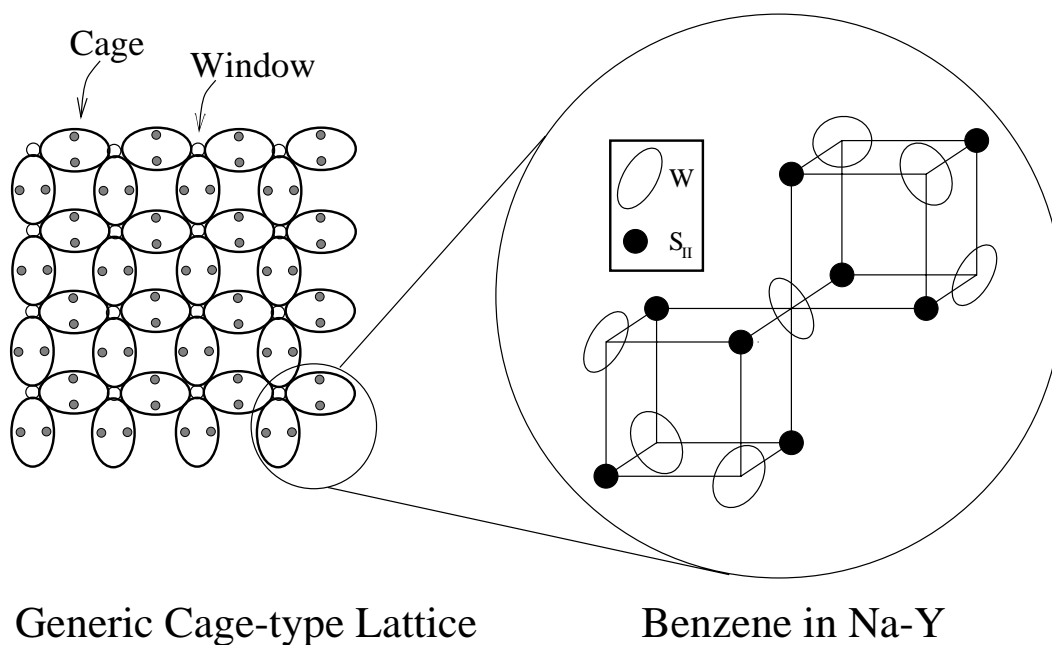


FIG. 5. Schematic lattice model for molecules in cage-type zeolites, showing cages, intracage sites and window sites (left), as well as the specific lattice geometry for benzene in Na-Y zeolite (right).

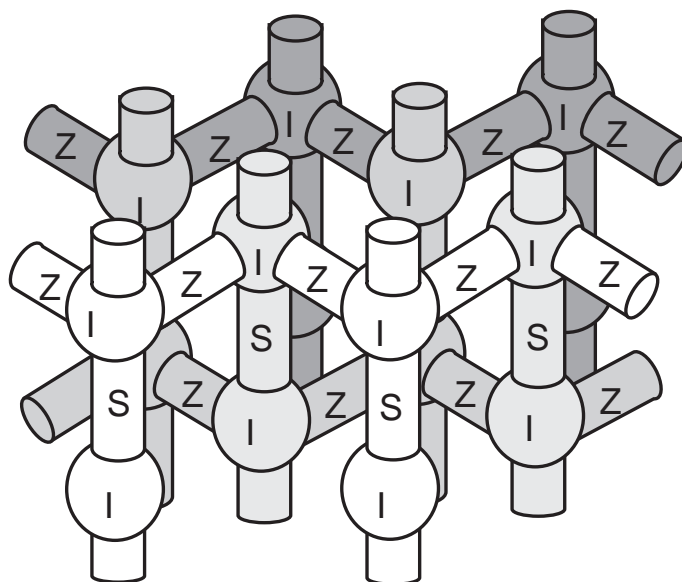


FIG. 6. Channel and site structure of silicalite-1 showing intersection sites (I), straight channel sites (S) and zig-zag channel sites (Z).

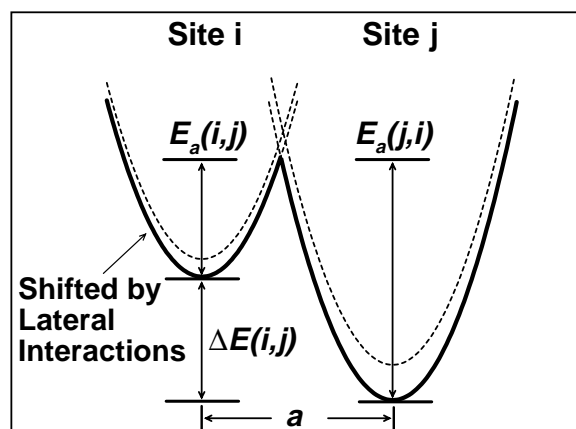


FIG. 7. Site-to-site jump activation energies perturbed by guest-guest interactions, approximated with parabolic jump model.

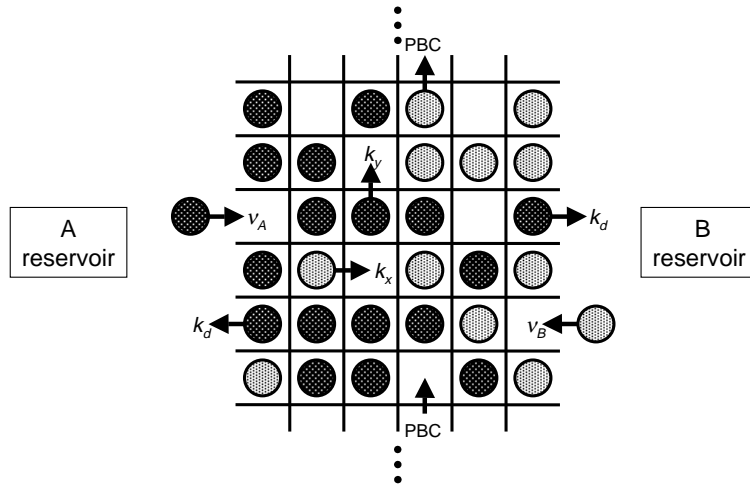


FIG. 8. Schematic of a tracer counter-permeation simulation, with identical but differently labeled particles. Diffusion anisotropy is controlled by the parameter $\eta = k_y/k_x$, with the limiting case $\eta = 0$ corresponding to single-file diffusion.